INVESTIGATION OF THE EFFECT OF SODIUM BUTYRATE INDUCED DIFFERENTIATION ON INFLAMMATORY PATHWAYS IN COLON CANCER CELLS

A THESIS SUBMITTED TO
THE GRADUATE SCHOOL OF NATURAL AND APPLIED SCIENCES
OF
MIDDLE EAST TECHNICAL UNIVERSITY

BY

MÜMİNE KÜÇÜKDEMİR

IN PARTIAL FULFILLMENT OF THE REQUIREMENTS
FOR
THE DEGREE OF MASTER OF SCIENCE
IN
BIOLOGY

JULY 2012

Approval of the thesis:

INVESTIGATION OF THE EFFECT OF SODIUM BUTYRATE INDUCED DIFFERENTIATION ON INFLAMMATORY PATHWAYS IN COLON CANCER CELL LINES

submitted by MÜMİNE KÜÇÜKDEMİR in partial fulfillment of the requirements for the degree of Master of Science in Biology Department, Middle East Technical University by,

Prof. Dr. Canan Özgen _____
Dean, Graduate School of Natural and Applied Sciences

Prof. Dr. Musa Doğan _____
Head of Department, Biology, METU

Assoc. Prof. Dr. Sreeparna Banerjee _____
Supervisor, Biology Dept., METU

Examining Committee Members:
Prof. Dr. Semra Kocabıyık _____
Biology Dept., METU

Assoc. Prof. Dr. Sreeparna Banerjee _____
Biology Dept., METU

Assoc. Prof. Dr. Mesut Muyan _____
Biology Dept., METU

Assist. Prof. Dr. Özlen Konu _____
Molecular Biology and Genetics Dept.,
Bilkent University

Dr. Erhan Astarcı _____
Biology Dept., OKU

Date: _____

I hereby declare that all information in this document has been obtained and presented in accordance with academic rules and ethical conduct. I also declare that, as required by these rules and conduct, I have fully cited and referenced all material and results that are not original to this work.

Name, Last name: Mümine Küçükdemir

Signature :

ABSTRACT

INVESTIGATION OF THE EFFECT OF SODIUM BUTYRATE INDUCED DIFFERENTIATION ON INFLAMMATORY PATHWAYS IN COLON CANCER CELLS

Küçükdemir, Mümine
M.Sc., Department of Biological Sciences
Supervisor: Assoc. Prof. Dr. Sreeparna Banerjee

July 2012, 77 pages

Sodium butyrate (NaBt) is a four-carbon short chain fatty acid, produced naturally in colon as the end product of the bacterial anaerobic metabolism on dietary fibers. It was previously shown that NaBt can induce differentiation and may inhibit proliferation. The objective of this study was to investigate the effect of NaBt-induced differentation on inflammatory pathways in HT29 colon cancer cells. For this purpose, first, cells were treated with varying concentrations of NaBt from 1-5 mM and amount required to induce differentiation was determined as 3 mM. To understand the effect of NaBt on inflammation, the NF-kappaB pathway (p50 and p65) was investigated. Immunofluorescent staining showed increased nuclear translocation of p50 subunit with no remarkable change in subcellular localization of p65; moreover a synergistic effect was observed when cells were co-treated with NaBt and an NF-kappaB repressor, Bay 11-7085; implying the formation of repressive p50 homodimers in the nucleus. Our preliminary chromatin immunoprecipitation results showed that p65 recruitment

to the promoters of ICAM-1 was reduced, whereas p50 recruitment was increased. However, analysis of NF-kappaB target genes showed that cells treated with 3 mM NaBt have higher expression of the cytokines IL1-β and TNF-α, adhesion molecules ICAM-1 and VCAM-1 but not COX-2. These results suggest that NaBt-induced differentiation could cause the emergence of an inflammatory signal in HT29 cells as an anti-tumor mechanism, independent from the NF-kappaB activity. This work will be important in understanding the role of SCFAs in the colon microenvironment and may provide alternative therapeutic options in colorectal cancer.

Key words: Sodium butyrate, colorectal carcinoma, differentiation, inflammation, nuclear factor kappa-B.

ÖZ

KOLON KANSER HÜCRE HATLARINDA SODYUM BÜTİRATLA İNDÜKLENMİŞ FARKLILAŞMANIN ENFLAMASYON YOLAKLARINA ETKİSİNİN İNCELENMESİ

Küçükdemir, Mümine
Yüksek Lisans, Biyolojik Bilimler Bölümü
Tez Yöneticisi: Doç. Dr. Sreeparna Banerjee

Temmuz 2012, 77 sayfa

Sodyum bütirat (NaBt), kalın bağırsak mikroflorasındaki bakterilerin besinsel lifleri anaerobik metabolizması sonucu doğal olarak üretilen, dört karbonlu bir kısa yağ zinciridir. Sodyum bütiratın proliferasyonu engellediği ve hücre farklılaşmasını tetiklediği daha önce gösterilmiştir. Bu çalışmanın amacı da HT29 kolon kanser hücrelerinde, sodyum bütirat muamelesi ile başlatılmış hücre farklılaşması sırasında enflamasyon yolaklarının araştırılmasıdır. Bu amaçla, ilk olarak HT29 hücreleri 1-5 mM arası değişen konsantrasyonlarda muamele edilmiş ve 3 mM konsantrasyonun farklılaşmanın başlatılması için yeterli olduğu gözlemlenmiştir. Sodyum bütiratın enflamasyon üzerindeki etkisini anlamak için NF-kappaB yolağı (p50 ve p65) incelenmiştir. Immünoflorasan boyama deneyleri sonucu p50 nükleer lokalizasyonunun artarken, p65 lokalizasyonunun sabit kalması, ek olarak gözlemlenen sodyum bütirat ve NF-kappaB baskılayıcı Bay 11-7085 etkileşimi, baskılayıcı p50 homodimer oluşumunu akla getirmiştir.

Kromatin immün çöktürme deneylerimizin ilk aşaması ICAM-1 promotor bölgesinde p65 bağlanmasının azalırken, p50 bağlanmasının arttığını göstermiştir. Diğer yandan, COX-2 haricindeki NF-kappaB hedef genlerinden sitokinler IL1-β ve TNF-α, tutunma molekülleri ICAM-1 ve VCAM-1 mRNA seviyelerinde, 3 mM NaBt muamelesi sonrası artış gözlemlenmiştir. Bu sonuçlar sodyum bütirat ile başlatılmış hücresel farklılaşmanın, HT29 hücrelerinde bir anti-tümör mekanizması olarak, enflamasyon sinyallerinde artışa sebep olabileceğini işaret etmektedir. Bu çalışma, kolon mikroflorasında kısa zincirli yağ asitlerinin etkilerinin anlaşılmasında önemli olacak ve kolorektal kanserde muhtemel terapötik alternatifler sunabilecektir.

Anahtar Kelimeler: Sodyum bütirat, kolorektal kanser, farklılaşma, enflamasyon, nükleer faktör kappa-B.

To Şerife Ata

ACKNOWLEDGEMENTS

Firstly, I would like to express my deepest gratitude to my supervisor Assoc.Prof Sreeparna Banerjee for her guidance, encouragement, support and comments throughout my study.

My sincere thanks go to all my dear lab friends together with whom working was a joy from the first day of my studentship at Lab-B59. Especially Aslı Sade, Seda Tuncay and Şeyma Ceyhan for their invaluable motivational and moral support even at most challenging situations; Erhan Astarcı for his outstanding inspirational guidance and the "brainstorming discussions"; Aslı Erdoğ and Shabnam Enayat for their sincere companionship throughout my study.

I would like to express my special thanks to Aslı Sade for her invaluable support in real-time PCR experiments as well.

This study was supported by a grant (110S165) and a bursary (111S308) from TÜBİTAK.

Finally, I am deeply grateful to my parents Eyüp and Hatice Küçüdemir and my dear brothers; for their encouragement, endless help, confidence and especially Mehmet Küçükdemir for his understanding and motivational support.

TABLE OF CONTENTS

LIST OF FIGURES

FIGURES

LIST OF TABLES

TABLES

CHAPTER 1

INTRODUCTION

"No organ in the body is so misunderstood, so slandered and maltreated as the colon"

Sir Arthur Hurst

1.1 Overview of Normal Colon Physiology

The colon, an approximately five feet-long hollow organ towards the terminal part of the gastrointestinal tract, functions in the reabsorption of water and electrolytes from the chyme and formation of faeces (Valeur and Berstad 2010). Furthermore, due to the fact that it houses the body's greatest microbial diversity in colonic microflora, it also contributes to the metabolism of complex carbohydrates, synthesis of B complex vitamins and vitamin K, development of mucosal barrier function as well as modulation of innate and adaptive immune responses via bacterial metabolites (Segata et al. 2012). Extending from the ileocecal valve to anus, it is composed of three main parts: ascending, transverse and descending colon, surrounded by sphincter muscles, as well as a rich vascular network and nerve supply.

Similar to intestinal mucosa, colonic mucosal lining also contains many lymphocytes and lymphatic nodules scattered in between enterocytes (absorptive epithelial cells) and goblet cells (mucus-producing endocrine cells). The epithelium forms crypts alongside the colon, but unlike intestinal anatomy, interior part of the colon appears flat with no villi (Fox 2008).

1.1.1 Colonocyte Differentiation

Colon is one of the organs in the body that has substantial self-renewal capacity with continuous turnover and shedding of epithelial cells accompanied by proliferating progeny replacing the inner lining. An estimate of average life-span of an epithelial cell in colon is determined as 4-8 days by a technique in which loss of tritium-labeled deoxyribonucleic acid was monitored in the colon of albino male mice by autoradiography (Lipkin 1965, Creamer, Shorter and Bamforth 1961).

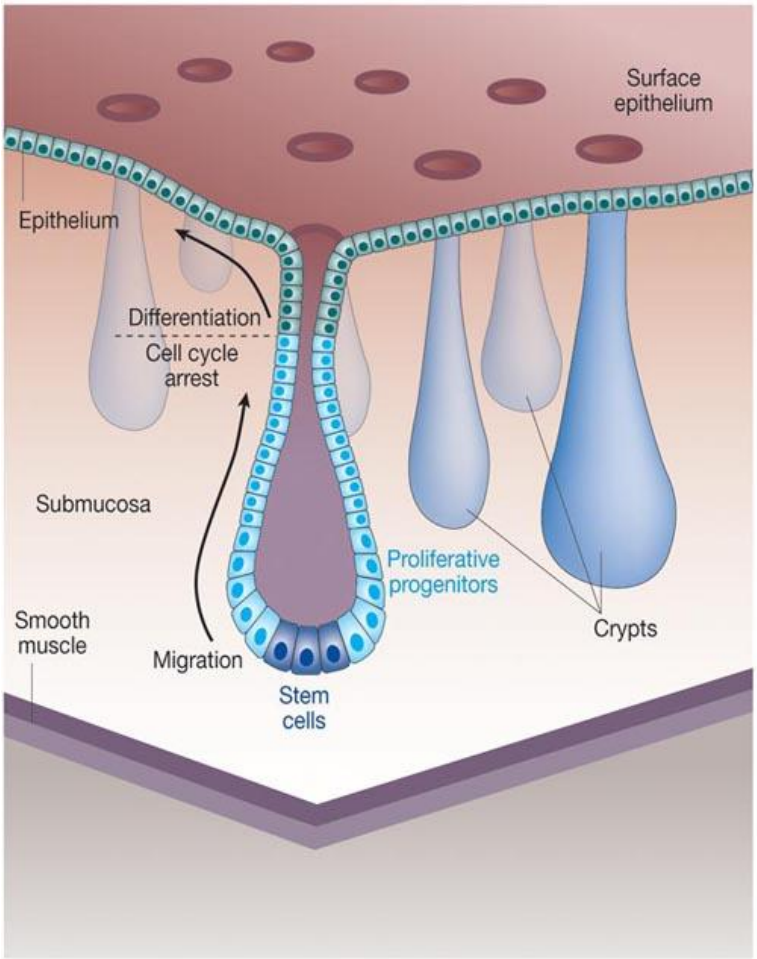

Figure 1.1 Tissue anatomy of the colonic epithelium. Image is retrieved from (Reya and Clevers 2005)

A general model suggested for the turnover of epithelial lining is as follows (Creamer et al. 1961, van der Flier and Clevers 2009) (Figure 1.1):

* Crypts, the invasions of epithelial lining into the underlying connective tissue, are the location for cell proliferation. Small, undifferentiated cells called as crypt base columnar (CBC) cells proliferate rapidly in the crypt base and give rise to transit amplifying cells.
* In a period of about one day, transit amplifying cells migrate towards the epithelial surface along the crypt.
* Once they reach to the epithelial surface, they are in a terminally differentiated state.
* Later in their life cycle, they undergo spontaneous apoptosis and shed into the colonic lumen.

Creamer et al. also suggested that reabsorption of cellular components might be taking place as they have observed accumulation of labeled particles in the periphery of the cytoplasm of the surface cells, after they have recorded diminished signal from nuclei of cells in the epithelial lining.

Typical cell lineages located from the top to the bottom in a colonic crypt are enterocytes and goblet cells, enteroendocrine cells, transit-amplifyying cells and CBCs respectively (Medema and Vermeulen 2011). Throughout their journey from the crypt base to the epithelial surface, several well-studied molecular events take place in the colonocytes.

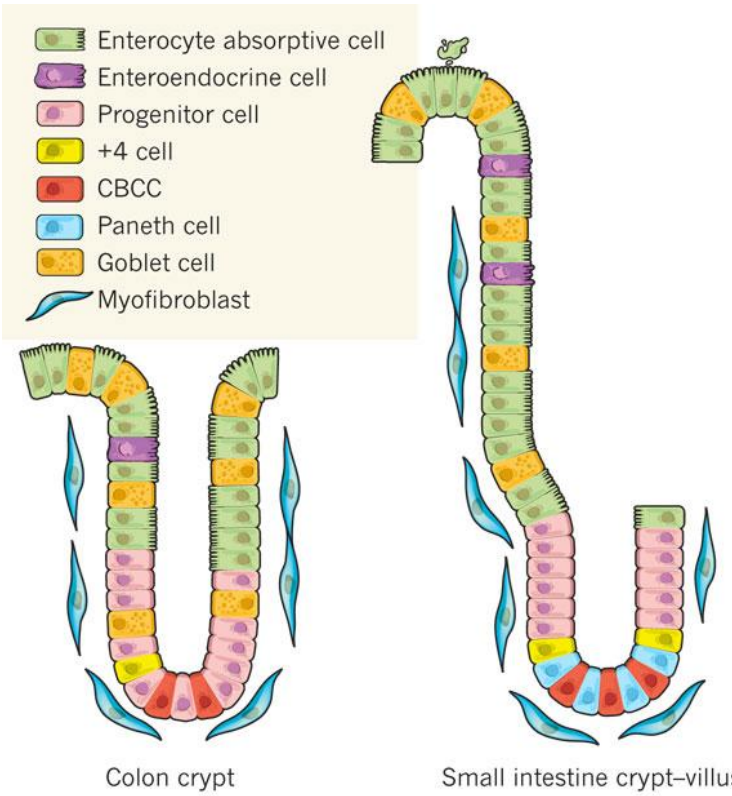

Figure 1.2 Comperison of cellular composition between colon crypt and intestinal crypt. Image is retrieved from (Medema and Vermeulen 2011).

The Wnt pathway is a significant player behind the proliferation of colon epithelia. Briefly, in the presence of Wnt ligand, which activates Frizzled and LRP transmembrane receptors, proteasomal degradation of β-catenin upon phosphorylation by APC degradation complex is inhibited. Active β-catenin translocates to the nucleus and transactivates Wnt target genes which were shown to be expressed in proliferative crypt progenitors (Kosinski et al. 2007). Research shows that expression of Wnt target genes follows a gradient pattern with the highest activity in the bottom of the crypt and downregulated towards the surface of colon epithelia. (Gregorieff et al. 2005)

Another highly conserved pathway that plays role in decisions on cellular fate in the course of colonocyte differentiation is the Notch pathway. In this pathway, interaction of Notch ligand with corresponding Notch receptors leads to the proteolytic cleavage of Notch intracellular domain (NCID) Free NCID translocates to the nucleus and activates target gene expression upon its interaction with some other transcription factors (Tamura et al. 1995).

Inhibition of Notch pathway during *in vivo* studies in mice resulted in the conversion of all epithelial cell population into goblet cells (van Es et al. 2005). On the other hand, mouse models of impaired Wnt signaling resulted in an epithelial lining phenotype composed solely of enterocytes. Lastly, it is also remarkable to note that unlike the Wnt signaling pathway, there are no mutation in the Notch pathway proteins are associated with colorectal tumorigenesis (van der Flier and Clevers 2009).

1.1.2 Colon Microbiota

The average adult body is composed of 100 trillion human cells. (Roza 2006) Besides this, human body is much widely (10 times more) populated by a variety of microbes consisting of eukaryotes, archaea, bacteria as well as viruses, which all together constitute the human microbiome. (Wenner 2007, Methe et al. 2012) For population scale investigation, the National Institutes of Health-funded Human Microbiome Project was launched in 2008 with the following aims:

- To identify a healthy human microbiome
- To detect shifts in microbial taxonomic and functional profile in health and disease conditions
- To provide a set of data for identification of new species
- To promote development of novel strategies for treatment making use of prebiotic species
- To develop a variety of protocols to enable a project of this scope.

Up to now, 5,298 samples from 15 (male) and 18 (female) body sites of 242 healthy individuals between the ages of 18-40 years have been processed in two clinical centers; Baylor College of Medicine (BCM) and Washington University School of Medicine. 16S rRNA, whole shotgun sequencing (WGS) and reference genome sequencing were carried out across four centers; BCM Human Genome Sequencing Center, The Broad Institute of Massachusetts Institute of Technology and Harvard, the J.Craig Venter Institute and The Genome Institute at Washington University School of Medicine. For storing the 3.5 terabases of data generated in this study, a Data Analysis and Coordination Center (DACC) was established. Detailed information on biological samples, clinical protocols, news, project statistics were stored in DACC as well. Sampling was done from human airways, skin, oral cavity, gut and vagina. Roche 454 FLX platform was adopted for the 16S sequencing protocol whereas the Illumina GAIIx platform with 101-base-pair-paired-end reads was used for WGS sequencing. Due to the presence of highly conserved sequences, 16S rRNA gene was quite informative for use in taxonomic classification.

In the scope of this project, several publications have been released on recent findings about the human microbiota. Segata et al. reported results of their research on composition of adult digestive tract in volume 13 of Genome Biology. (Figure 1.3) Following a metagenomic research they have carried out on stool samples, it was found that over 60% of microbiota was composed of Bacteroidetes; second most populated genus was Firmicutes. Proteobacteria, Acinobacteri and Fusobacteria species were also detected in stool samples with a very low relative abundance. In addition, Porphyromonadaceae family of pathogens, Parabacteroides, Barnesiella, Odoribacter and Butyricimonas were most prominent species identified in stool. After identifying species colonizing various sites of digestive tract, they have also performed an analysis to associate metagenomes with metabolic modules related with different body sites. For both

upper and lower digestive tract, iron transporters and pathways playing role in H_2 and H_2S production was observed to be common (Segata et al. 2012).

In the light of most recent findings, $1x10^{11}$ bacterial cells per day are estimated to be flowing through the digestive tract from mouth to the stomach. (Socransky and Haffajee 2002, Richardson and Jones 1958) However, research is still ongoing to investigate whether there exists a link between microbiota of distinct sites of digestive tract and whether distal sites of the tract are seeded by oral microbiota.

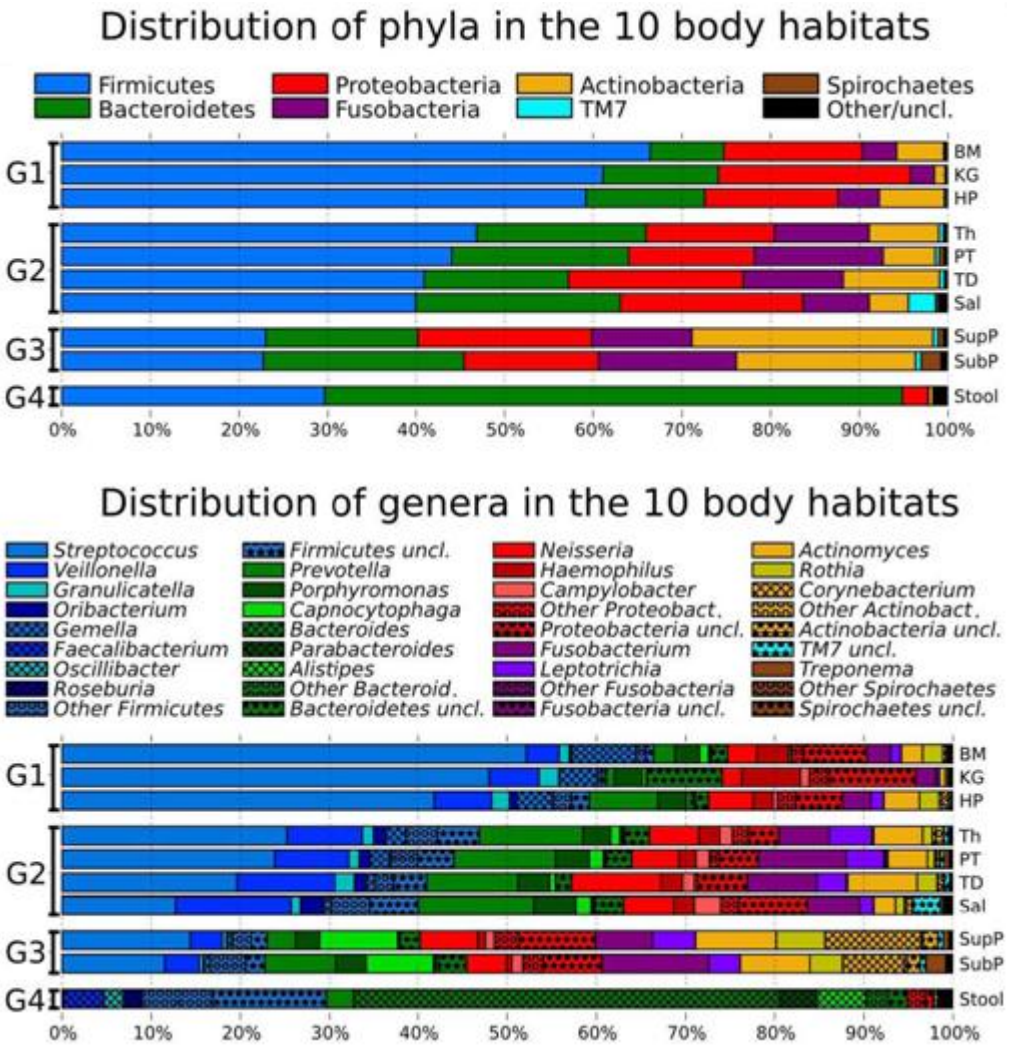

Figure 1.3: Groups detected in the sampled digestive tract microbiome sites based on similarities in microbial composition. Taxonomic composition of the microbiota in the ten digestive tract body habitats investigated based on average relative abundance of 16S rRNA pyrosequencing reads assigned to phylum (upper chart) and genus (lower chart). Microbiota from the ten habitats are grouped based on the ratio of Firmicutes to Bacteroidetes as follows: Group 1 (G1), buccal mucosa (BM), keratinized gingiva (KG) and hard palate (HP); Group 2 (G2), throat (Th), palatine tonsils (PT), tongue dorsum (TD) and saliva (Sal); Group 3 (G3), supraginval (SupP) and subgingival plaques (SubP); and Group 4 (G4), stool (Stool) (Segata et al. 2012).

1.2 Colorectal Cancer

1.2.1 De-differentiation and Neoplastic Progression

Loss of specialized properties and revert-back of cellular fate to a lesser differentiated stage within its own lineage is called dedifferentiation. In some cases, a change in cellular phenotype to a more unspecialized state can also be considered as a trouble-shooting mechanism of a differentiated cell to be able to survive under unfavorable conditions. To illustrate, cells can shift their metabolism to adapt to anaerobic conditions in case of insufficient oxygen supply and thus, under such conditions energy metabolism becomes more dependent on glycolytic pathway instead of oxidative metabolism which is also typical of an undifferentiated phenotype (Horne 1992). Together with the gain of undifferentiated properties, the proliferative potential of cells increases substantially. In the end, loss of specialized features and unrestrained growth capacity leads to malignant transformation. Dedifferentiation of specialized colonocytes might be followed by the adenoma-carcinoma sequence suggested for colorectal tumorigenesis (Fearon and Vogelstein 1990).

Neoplastic progression of colorectal malignancy is explained under four main stages according to the adenoma carcinoma model (Figure 1.4, Figure 1.5):

- Earliest detectable lesions of adenoma, in either sporadic CRC (colorectal acrcinoma) or FAP (familial adenomatous polyposis), lacks APC (adenomatous polyposis coli) gene expression.
- KRAS (Kirsten rat sarcoma viral oncogene homolog) mutations are detected in about 50% of intermediate and late adenomas, but 10% in early adenomas suggesting that it is involved in a later stage.

- Loss of heterozygosity on q arm of chromosome 18 is observed in about 50% of late adenomas, whereas assigned candidate genes to this region are DCC (deleted in colorectal cancer) and SMAD4 (mothers against decapentaplegic homolog 4).
- Biopsy samples isolated from patients with colon carcinoma mostly observed to have TP53 mutations whereas in adenomas this mutation was not observed.

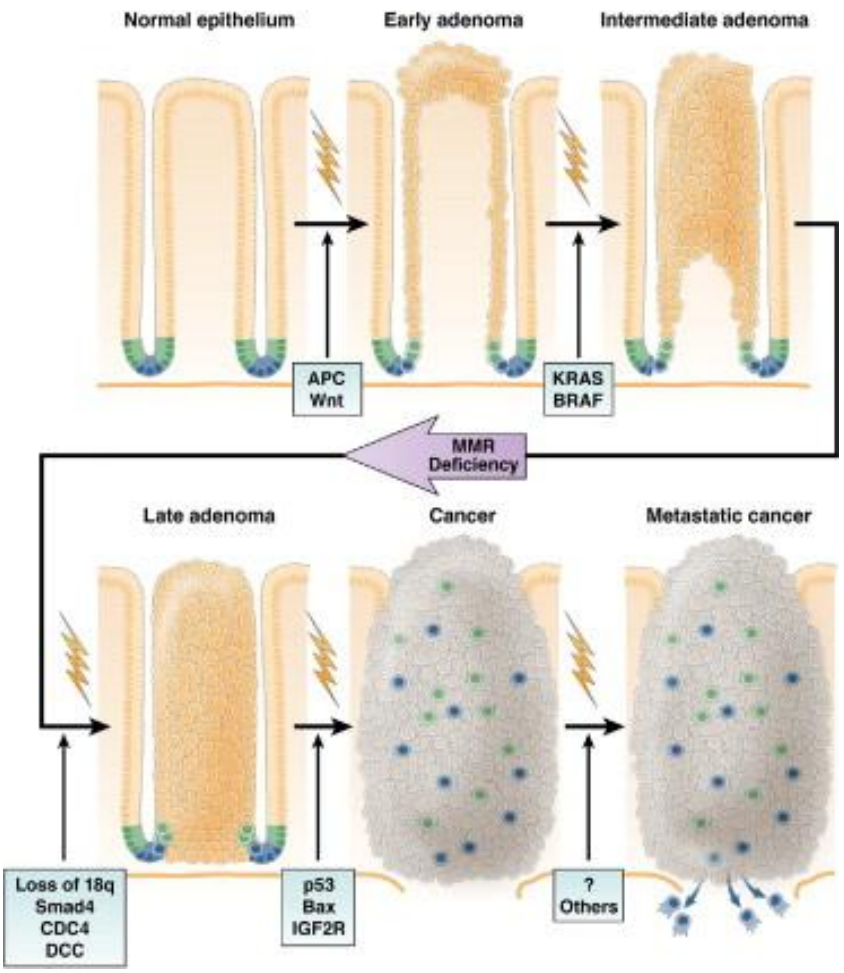

Figure 1.4 Schematic presentation of the development of colon carcinoma. Image is retrieved from (Todaro et al. 2010)

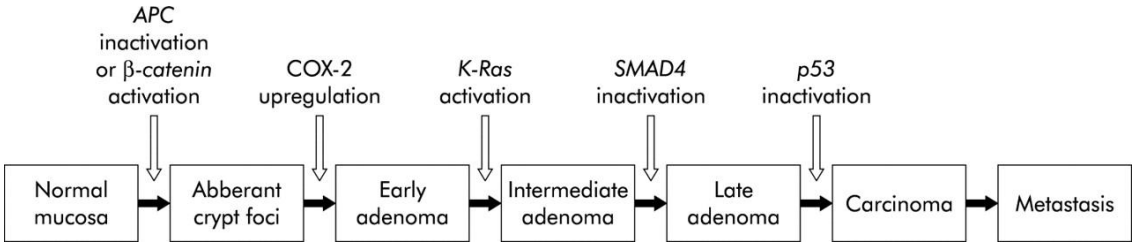

Figure 1.5 Schematic representation of adenoma-carcinoma sequence model. Image is retrieved from (Brosens et al. 2005).

1.2.2 In Vitro Models of Differentiation

De-differentiation of specialized colonocytes starts with malfunctioning in some cellular pathways (e.g. APC/Wnt) that are normally involved in differentiation of progenitor cells residing in the colonic crypts as explained in Section 1.1.1; and finally leading to fully specialized cells to gain a more unspecialized phenotype. Under laboratory conditions, it is possible to generate *in vitro* models of differentiation for colonocytes using colorectal cancer cell lines which are accompanied by relevant functional and morphological alterations. To illustrate, spontaneous-differentiation models of Caco-2, T84 and HT29 cell lines are available (Astarci et al. 2012, Niv et al. 1992, Fantini et al. 1986). In these differentiation models, colon cancer cell lines are grown to confluency in culture flasks and during the days of post-confluency, cells are checked for their differentiation status. Another model includes treatment of colorectal cancer cell lines in culture conditions with some chemical inducers of differentiation such as sodium butyrate, sodium suramin, trichostatin A, retinoic acid, resveratrol, etc (Mayo et al. 2007, Tureckova et al. 2005, Reynolds, Rajagopal and Chakrabarty 1998, Wolter and Stein 2002). Differentiation status of cells in these *in vitro* models are characterized by gain of a differentiated morphology marked by the development of tight junctions between neighboring cells, gaining brush-border membrane or domes; as well as the expression of some colon specific proteins

such as structural proteins like villin or enzymes like alkaline phosphatase (IAP), dipeptidyl-peptidase and sucrase isomaltase (Pinto et al. 1983)

Among the differentiation markers used in colon cancer research, it is important to note that the isoenzyme of alkaline phosphatase of intestinal origin is used to validate differentiation whereas some other isoenzymes of alkaline phosphatase are also known to be used as a tumor marker, especially placental alkaline phosphatase (Koshida et al. 1991). All alkaline phosphatase isoenzymes are membrane glycoproteins containing neutral hexose groups and hexosamines. Among three types of alkaline phosphatases, namely, hepatic, intestinal or placental origin, only intestinal alkaline phosphatase lacks sialic acid in its structure which may potentially be responsible for its distinct functional properties compared to the other two isoenzymes (Jardillier 1981). It has been suggested that sialic acid, by creating a negative surface charge on cellular membranes may lead to the emergence of repulsive forces between cells and enhances metastatic potential of later-stage cancers, proven by the presence of high density of sialic acid-rich glycoproteins expressed on the surface of metastatic cells (Fuster and Esko 2005). Therefore, the increased expression of IAP, which lacks the sialic acid modification, in the differentiated cells is unlikely to be a marker of neoplastic progression.

These *in vitro* models have been utilized in colorectal cancer research for years for a better understanding of the molecular events behind the process of cellular differentiation, transepithelial migration studies as well as malignant progression (Reynolds et al. 1998, Niv et al. 1992)

1.3 Inflammation

Inflammation is the term used to identify a series of complex biological response collectively against a damaging stimulus as a mechanism of innate immunity. Four main symptoms used to identify an inflammatory response are pain (dolor), fever (calor), redness (rubor) and swelling (tumor) (Abbas and Lichtman 2009).
In a normal inflammatory response, owing to the presence of a negative-feedback loop, release of pro-inflammatory cytokines is followed by production of anti-inflammatory cytokines. Thus, in the site of injury, inflammation does not last long. On the other hand, if the mechanisms that play role in resolution of inflammation are defective, continuing activity of pro-inflammatory signals may lead to the emergence of chronic inflammation (Coussens and Werb 2002).

1.3.1 Inflammation-Related Cancers

As explained in Section 1.2.1, colorectal tumor initiation starting with the first mutation should be accompanied by several other mutations to promote malignancy. Taking the crypt morphology into account, the host of the first mutation should be either a stem cell in the crypt base or a transit amplifying cell that would have sufficient time to acquire the later stage mutations following the first hit. Life-span of a differentiated colonocyte in the epithelial lining would less likely to be long enough to acquire all these mutations for neoplastic progression (Grivennikov, Greten and Karin 2010). On the other hand, there might be some factors that promote the occurrence of somatic mutations which play substantial roles in cancers that usually originate from sporadic mutations rather than germline mutations.

Chronic inflammation is such a factor that makes tumor microenvironment more favorable for its growth. There two main mechanisms suggested for inflammation-cancer relationship.

- Risk of developing cancer may increase due to the persistence of chronic inflammation. Reactive oxygen and nitrogen species produced by inflammatory cells can be regarded as potent mutagens since they may cause DNA damage and mutations. Moreover, leukocytes recruited to the area of inflammation through secretion of some cytokines and chemokines may provide growth-stimulating factors to the neoplastic cells at the later stages of tumorigenesis. Persistent H.pylori infection associated with gastric cancer, Hepatitis B infections associated with hepatocellular carcinoma and Schistosoma and Bacteroides infections associated with colon cancer constitutes examples to this type of inflammation-related cancers.
- Secondly, inflammation may develop at a later stage following the tumor development. To illustrate, lung cancer may promote inflammation by secreting molecules that activate macrophages through TLR 2 receptors and enter into a cycle of continuous self-renewal and proliferation. Besides this, cancer therapy might induce inflammation as well due to the necrotic cell death and thereby the release of inflammatory mediators caused by radiotherapy or chemotherapy (Morgan, Forssman and Nakada 2004).

The chronic inflammation-induced model of colorectal cancer suggested more than a century ago by Rudolf Virchow has gained much more importance over the adenoma-carcinoma sequence model throughout the years as 95% of all colorectal cancers are shown to be caused by sporadic mutations whereas germ-line mutations account for 5% of the cases (Meng et al. 2012, Balkwill and Mantovani 2001)

1.3.2 The NF-kappaB Pathway

NF-kappaB is an eukaryotik transcription factor which binds to the decameric consensus sequences (5'-GGGRNWYYCC-3') on DNA in response to several exogenous stimuli such as UV, shear stress, ROS, double stranded RNA, IL1-β, TNF-α and LPS (Sen and Baltimore 1986) (Figure 1.6). NF-kappaB family of proteins are characterized by a 300 amino acid region in their N-terminal domain which comprises DNA binding domain, dimerization domain and a nuclear localization signal, all together called as Rel-homology domain (RHD).

According to the ability of transactivation, members of the NF-kappaB family can be divided into two categories. Those that have a transactivation domain at their C-terminus are Rel proteins; p65 (RelA), RelB and c-Rel. The other two members, p50 and p52, lack the transactivation domain (Ghosh 2007). Instead, they have 6-7 ankyrin repeats at their C-terminus when they are first synthesized as 105 kDa and 100kDa precursors. This C-terminus region of p105 and p100 shows homology with IkB family of proteins (Sedgwick and Smerdon 1999). Furthermore, both p105 and p100 can interact with the RHD of Rel proteins (p65, RelB or c-Rel) via these ankyrin repeats as IkB members do and inhibit nuclear localization by masking the nuclear localization signal of their target;. Thus, p50 and p52 precursors can inhibit NF-kB transcriptional activity. Moreover, if these two NF-kappaB members (p50/p52) dimerize and occupy kappaB consensus sequence on DNA, they may also hinder NF-kappaB transcriptional activation by preventing p65, c-Rel or RelB recruitment to these sites (Ghosh 2007) (Figure 1.6, Figure 1.7).

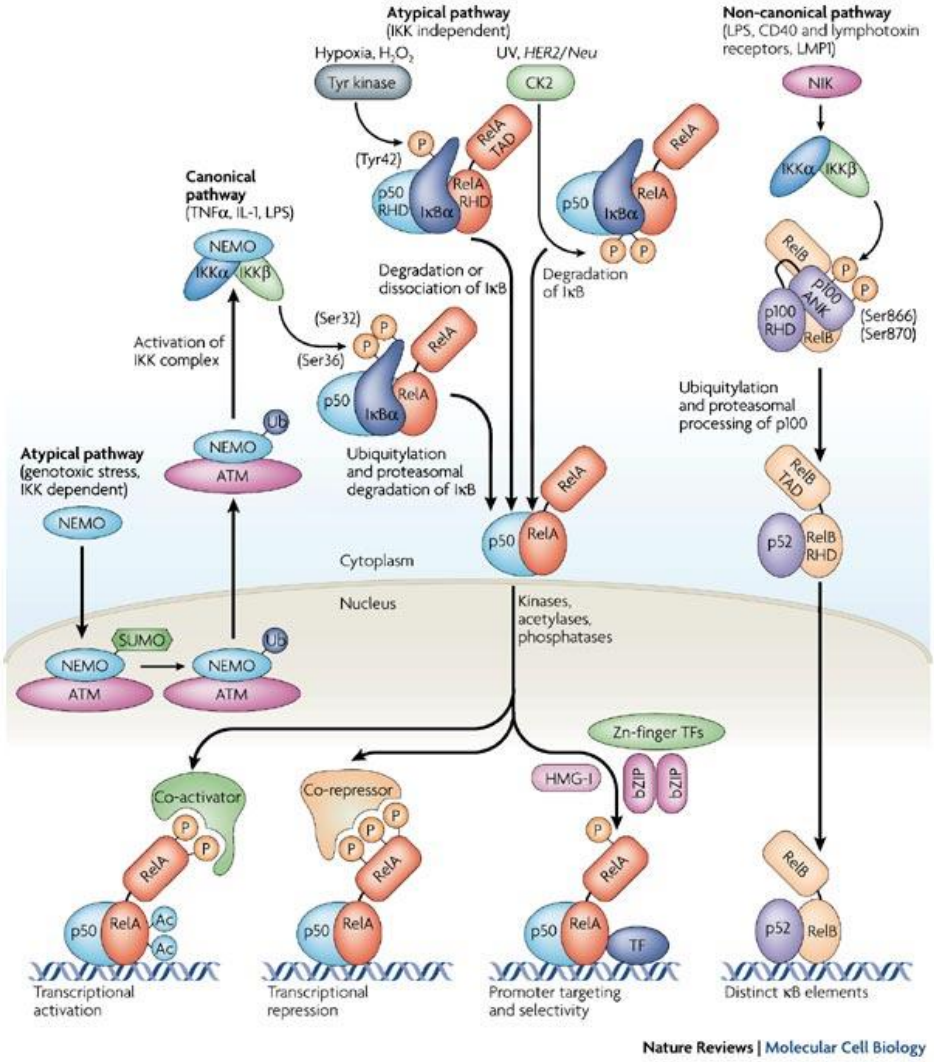

Figure 1.6 Pathways leading to the activation of NF-kappaB . Image is retrieved from (Perkins 2007)

Subcellular localization of the NF-kappaB subunits is important for the regulation of NF-kappaB activity and this regulation is achieved by Inhibitor of NF-kappaB (IkB) family of proteins (Baeuerle and Baltimore 1988). IkB family of proteins are composed of eight members that share multiple ankyrin repeats at their C-terminus. Each IkB protein has a preferential target of NF-kappaB/Rel dimers for inhibition. To illustrate, IkBα/β preferentially interacts with complexes that have either Rel A or c-Rel and prevent their nuclear localization (Huxford et al. 2002).

Special targets of Bcl3 and IkBζ are usually homodimers of p50 or p52. IkBε has the potential to inhibit homodimers of c-Rel and Rel A (Li and Nabel 1997, Simeonidis et al. 1997, Whiteside et al. 1997). Finally, the p50/p52 precursors, p100 and p105 respectively, do not show high selectivity among NF-kappaB/Rel dimers.

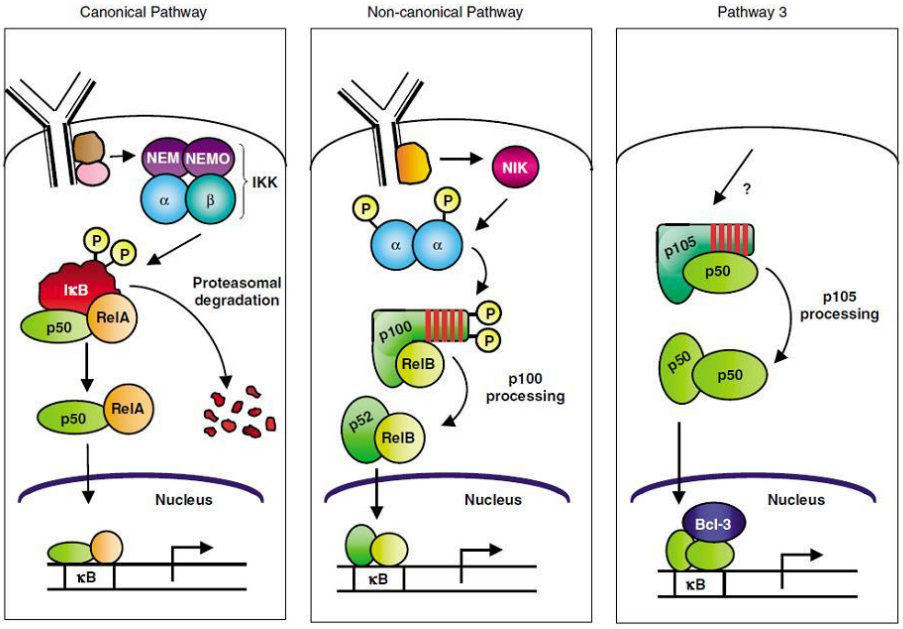

Figure 1.7 Pathways leading to the activation of NF-kappaB. Image is retrieved from *http://www.mbc.manchester.ac.uk/research/NFkB/NFkB.html*

Signals that control IkB/NF-kappaB interaction is provided by Inhibitor of kappa B kinase (IKK) protein complex upstream of IkB. IKK complex is composed of three subunits that are namely IKKα, IKKβ and IKKγ which makes up a 900kDa unit. The NF-kappaB canonical pathway is mainly regulated by IKKβ which is both necessary and sufficient for IKBα/β phosphorylations (Ghosh 2007). There is little known about the effect of IKKα on the canonical pathway. However, regulation of the non-canonical pathway is solely dependent of IKKα. IkB phosphorylation by IKK complex is a signal for ubiquitinylation of IkBs which are then degraded in the proteasome. NF-kappaB/Rel dimers are released by the

removal of IkB proteins and upon nuclear localization, start their transcriptional activity (Senftleben et al. 2001).

NF-kappaB family of proteins were discovered in the course of immunological studies and has been investigated for their role in the immune system (Sen and Baltimore 2006). Later, the expression and activation of NF-kappaB members were investigated for their role in several stages of immune responses. The role of the NF-kappaB pathway in barrier function, which is the most conserved host defense mechanism, was elucidated in a study using transgenic mice deficient in I-kappaB generation which resulted unexpectedly in a thickened skin phenotype. Later, it was shown that p65 was responsible for the terminal differentiation of keratinocytes by inducing expression of epidermal differentiation genes (Banno, Gazel and Blumenberg 2005, Beg et al. 1995, Seitz et al. 1998). Moreover, NF-kappaB orchestrates the recruitment of an inflammatory response as well as resolution phase of inflammation and cells of innate immune system require NF-kappaB for their survival in the periphery, for avoiding activation of apoptotic program, especially during exposure to proinflammatory stimuli. Likewise, survival mechanism of cellular components of adaptive immune system also depends on NF-kappaB-regulated anti-apoptotic gene expression (Ghosh 2007). However, different from most of the other tissues, adaptive immune system organs are dependent on RelB for constitutive NF-kappaB activity, thereby on a signaling pathway mediated by RelB:p52 complexes and not the canonical p65:p50 heterodimer (Weih et al. 1995). Many human cancer cell lines and isolated tumor samples have been observed to have a constitutively active NF-kappaB pathway which is also known to be involved in chemokine dysregulation in cancers. Thus, NF-kappaB is a potential target at the crossroad of inflammation and carcinogenesis (Morgan et al. 2004).

1.3.3 Inflammatory Signaling in Cancer Cells

As explained at the beginning of section 1.3, activation of an inflammatory signal in a normal cell may be regarded as an alert for biological damage such as infection, injury, cellular stres conditions, etc. However, upregulation of inflammatory markers should not be interpreted similarly in normal cells and neoplastic cells. Upregulation of such a signaling mechanism, may lead to the activation of immunosurveillance mechanism marked by increased cytokine expression for recruitment of more leukocytes to the tumor site, upregulated expression of leukocyte adhesion molecules to enable immunological synapse, decreased generation of factors playing role in immune suppression in cancer patients.

To illustrate, ICAM-1 expression in colon adenocarcinoma cells were associated with an activated immunosurveillance system evoked against non-self tumor cells (Kelly et al. 1992). ICAM-1 (intercellular adhesion molecule 1) protein is an immunoglobulin superfamily member expressed on vascular endothelial cells as well as intestinal microvilli (Carpen et al. 1992, Frank and Lisanti 2008) and an integrin binding protein that can mediate heterophilic cell-to-cell adhesion upon its interaction with LFA-1 on the surface of lymphocytes. LFA-1 (Lymphocyte function associated antigen-1), being a leukocyte integrin marked with a common β-chain in its structure is expressed on T-cells, B-cells, macrophages and neurophills (Shaw et al. 2004). In the course of rolling, adhering and diapedesis stages of transepithelial migration, it ensures the firm adhesion following the first lymphocyte-endothelial cell interaction mediated by selectins (Janeway et al. 2004). In a study, blocking ICAM-1/LFA-1 interaction with antibodies reduced the interaction of lymphocytes with HT29 colorectal cancer cells (Kelly et al. 1992). Furthermore, another study conducted on resected colon adenocarcinoma tissue from 96 patients showed that higher number of tumor-infiltrating

lymphocytes (TIL) were found in ICAM-1 positive tumors and lymph node and liver metastasis were significantly lower in these tumors (Maeda et al. 2002).

Therefore, it is important to interpret inflammatory status of cells accurately by considering the metabolic profile and proliferative potential of cells as well as the state of cellular microenvironment.

1.4 Colorectal Cancer and Short Chain Fatty Acids

According to 2012 records of American Cancer Society, colorectal cancer is the third most common cancer type for both sexes although risk of developing CRC seems to be slightly higher in men than in women (http://www.cancer.org/). A report issued by the American Institute for Cancer Research (AICR) in 2007 indicates that an average of 34% of all cancers in general and 45% of CRCs can be prevented by following a healthy lifestyle (http://www.aicr.org/reduce-your-cancer-risk/cancer-prevention/reduce_cancer_by_numbers.html).

Most of the risk factors for developing CRC are dependent on living habits. People having a history of colon polyps, colorectal cancer, inflammatory bowel disease or type II diabetes are more likely to suffer from CRC. There are also some hereditary factors that are in close association with CRC dignosis. Familial adenomatous polyposis (FAP) caused by mutations in the APC gene and hereditary non-polposis colorectal cancer (HNPCC) caused by inherited mutations on multiple genes that play key role in DNA damage repair mechanism are the two most common syndromes. Moreover, risk of CRC diagnosis can be affected by age and different ethnic background (American Cancer Society, 2012).

In contrast to these inherited conditions, life-style related risk factors can be eliminated. First of all, these include following a healthy diet rich in fibers and low in saturated fats and simple sugars. Besides, high proportion of red-meat and processed meat products in diet are also associated with CRC. Next, being physicallly active and ensuring weight control, avoiding smoking and reducing alcohol consumption are also important precautions to prevent CRC (American Cancer Society, 2012).

1.4.1 Short-Chain Fatty Acids (SCFA): Production, Absorption and Utilization

The indigestable portion of foods is composed of two main components; namely soluble fiber and insoluble fibers (Agriculture 2005). Although resistant to digestion in the intestine, soluble fibers can be partially or completely fermented in the large bowel by the action of anaerobic colonic microbiota and give rise to short-chain fatty acids (SCFA) (Cummings 1981, Gibson and Roberfroid 1995) (Figure 1.8). According to the recent findings, Bacteroidetes are found to be the major producers of SCFA. There are studies indicating endogenous SCFA production by mammalian tissues as well, as a result of long-chain fatty acid catabolism by acetyl-CoA-dependent oxidation, although this hasn't been shown as the major source of butyrate in human body (Lehninger, Nelson and Cox 1993, Kien, Chang and Cooper 2000).

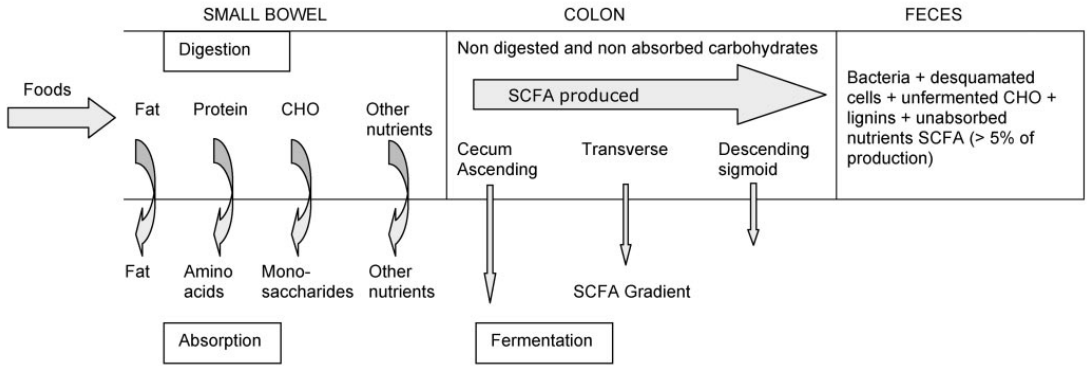

Figure 1.8 Overall scheme of nutrients in their transit through the GI tract. Image is retrieved from (Roy et al. 2006)

The highest rate of SCFA production takes place in the ascending colon and as it is readily absorbed upon production, luminal concentration dramatically decreases towards the distal sites of the organ. In the course of absorption, SCFAs can be either transported actively by an apical carrier mediated transport or passively by non-ionic diffusion through the apical membrane. Active transport of SCFA can be mediated by sodium-coupled monocarboxylate transporter in which ionized form of SCFA is exchanged with HCO_3^- ion. However, under the acidic conditions of colon (pH 5.5-7.5), SCFAs (pK_a: 4.8) are mostly found in the protonated form and they are readily transported by non-ionic diffusion rather than the active transport (Roy et al. 2006).

Colon has the highest concentration of SCFAs in human body. Concentration of SCFAs in colon lumen varies in between 20-140 mM. As a result of anaerobic fermentation 60% of the total SCFA production yields acetate, 20% gives rise to butyrate and the rest is the propionate. Among those, most of the butyrate is readily absorbed and used up in colon as the major energy source for nourishment of colonocytes. Rest of the SCFAs leave colon and enter the liver via portal venous system. Liver takes up most of the propionate and acetate is distributed to the peripheral circulation to be used by peripheral tissues. Therefore, regarding the

SCFA in bloodstream acetate concentration is the highest in peripheral circulation whereas butyrate concentration does not exceed 1-4 μM (Wong et al. 2006, Topping and Clifton 2001, Wolever et al. 1997).

1.4.2 Sodium Butyrate (NaBt)

Sodium butyrate is an SCFA composed of a 4-carbon aliphatic chain (Figure 1.9).

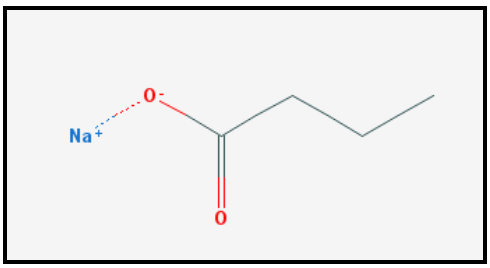

Figure 1.9 Chemical structure of sodium butyrate (PubChem Compound)

As stated earlier NaBt serves as the major energy source of colonocytes upon its β–oxidation inside the cells. Interestingly, whereas NaBt supports the proliferation of colonocytes as the primary energy source, its anti-proliferative effect on colorectal carcinoma cells has also been reported in a number of independent studies. It was shown to cause growth arrest, differentiation and apoptosis in colon cancer cell lines (Pool-Zobel 2005, Tureckova et al. 2005, Cohen, Ophir and Shaul 1999). Anti-tumorigenic effects of NaBt were also attributed to its ability to inhibit Class I and II histone deacetylases (HDACs) (Kim and Bae 2011, Davie 2003). Acetylated histones lead to chromatin relaxation due to the disrupted interaction between positively charged lysine tails and negatively charged DNA backbone. Therefore, upregulation of transcriptional activity takes place (Wanczyk et al. 2011).

Moreover, non-histone substrates of HDACs outnumber the histone targets and in a study, it was also shown that in Caco-2 cells butyrate can play role in acetylation status of non-histone substrates of HDACs (Chen et al. 2001, White et al. 2006).

Yet another way by which NaBt exerts its effect in colon microenvironment is via immunomodulatory routes. Butyric acid salt acidifies the colonic lumen and plays a protective role by preventing pH-sensitive pathogens such *as E.coli, Campylobacter and Salmonella* to populate the colon mucosa (Chen and Walker 2005). Furthermore it favors the colonization of health promoting bacteria such as Bactobacilli, Fusobacteria and Bifidobacteria (Roy et al. 2006). It was already suggested in a report submitted by Maslowski et al. that;

- Depending on the diet they follow, distinct populations may have quite different gastrointestinal microbiomes.
- Differences in the composition of microbiota can be reflected in different metabolic and immunologic responses of individuals.

Supporting this notion, studies were conducted on mice fed with a diet that is low in fat, rich in dietary fibers. Just 24h after switching to a typical western diet (rich in saturated fat and simple sugars) from the healthy diet, alterations were observed in the composition of colonic microbiota, furthermore reflections of this change was also observed in metabolic pathways simultaneously (Turnbaugh et al. 2009).

Another immunomodulatory effect of NaBt is explained by enhanced-danger signal hypothesis that may result in a robust innate immune response in the course of infection. Along with health-promoting microbiota, pathogenic bacteria are also capable of producing SCFAs and at the sites of infection concentrations may

reach to millimolar levels. Since the mechanism of first line of defense by immune system (inflammation or innate immune response) depends on the common pathological patterns such as presence of microbial metabolites at certain concentrations or bacterial surface molecules, secretions and proteins, presence of a threshold SCFA level may provide a much rapid response in case of a potential infection which will add up to the SCFA concentrations at the sites of infection (Janeway et al. 2004, Garland 2011, Vinolo et al. 2009).

Previously, it was shown that NaBt has an anti-inflammatory effect exerted via its inhibitory action on NF-kappaB in Crohn's disease (Segain et al. 2000). Moreover, there are published data on the inhibitory effects of NaBt on NF-kappaB pathway in colorectal cancer cell lines suggested to be governed by histone relaxation through histone deacetylase inhibition (HDACi) activity of NaBt; although there exists contradictory data on decreased NF-kappa activity via non-histone substrate effect of HDAC enzymes on Rel A subunit acetylation as well (Canani et al. 2011, Bocker et al. 2000, Chen et al. 2001).

Although NaBt is not a proven anticancer agent used in therapy, study conducted in 2003 showed that doubling of dietary fiber intake was associated with reduced risk of CRC by 40% (Bingham et al. 2003) Collectively, either on its immunomodulatory effects or anti-proliferative and differentiation-inducing effects, accumulation of promising data throughout the years on the potential benefits of NaBt in colorectal cancer may promote its usage as an alternative therapeutic approach.

1.5 Aims of The Study

Based on the recent explosion of research on the human microbiome, a study of bacterial fermentation products and its role in the modulation of cellular differentiation and inflammation is timely and very relevant. In this study, we have aimed to understand the effect of treatment of HT-29 CRC cells with NaBt on the NF-kappaB pathway and its target genes. According to our findings, 3 mM NaBt, which is determined as the sufficient concentration required to induce differentiation, leads to increased nuclear localization of p50 subunit of NF-kappaB whereas subcellular localization of p65 subunit remains unchanged. Although, this data showed implications of suppressed NF-kappaB activity, NF-kappaB target gene expression was observed to be increased for IL1-β, TNF-α, ICAM-1 and VCAM-1. All of the inflammation-related genes investigated in the scope of this study have kappaB binding sites in their promoter regions; however, only COX-2 gene expression indicated a parallel expression pattern with reduced NF-kappaB activity. We interpret this new expression pattern in HT29 cells in response to NaBt with an immunosurveillance model. In the light of our findings, we hypothesize that NaBt prevents the neoplastic progression with suppressed COX-2 expression and leads to the emergence of an inflammatory signal in HT29 cells, thereby enabling leukocyte migration to the site of tumorigenesis and evoking an adaptive immune response against cancer. Mentioned preliminary data is provided in Section.3 of this work; further investigation required to support our hypothesis will be carried out in our future studies.

CHAPTER 2

MATERIALS AND METHODS

2.1 Chemicals and Biological Reagents

Sodium butyrate (B5887) was purchased from Sigma-Aldrich, USA. 100 mM stock solution of it was prepared freshly in tissue culture grade PBS and was stored at +4°C up to 1 week.

Bay 11-7085(#1743) was purchased from Tocris Biosciences, Bristol, UK. 100 mM stock solution of inhibitor was prepared in DMSO and single-use aliquots were stored in -80°C for future use.

TNF-α recombinant protein expressed in E.coli (01-164) was purchased from Upstate, NY. 100ng/µl stock solution was prepared in MilliQ water, single-use aliquots were kept at -80°C until use.

2.2 Cell Culture

HT29 cells were purchased from Şap Enstitüsü, Ankara, Turkey and maintained according to the ATCC guidelines. McCoy's 5A medium (Biochrom AG, Germany) supplemented with 10% FBS, 2 mM L-glutamine and 1%

Penicillin/Streptomycin was used for culturing HT29 cells. Growing cells were maintained in an incubator supplying 95% humidity, 5% CO_2 at 37°C .

2.3 RNA Isolation and Measurement

For RNA isolations $3x10^5$ cells were seeded on 6-well-plates two days ahead of the treatment. Cells were treated with varying concentrations of sodium butyrate from 1 mM to 5 mM dissolved in cell culture grade PBS. Forty eight houts after treatment, total RNA isolation was carried out from cell lysates by using Qiagen RNeasy Minikit (Qiagen, USA) according to the manufacturer's guidelines . The integrity of the isolated RNA samples were checked by running 3µl of sample in 1% agarose gel and concentration measurements were carried out by using Nanodrop 2000 (Thermo,USA). Values calculated from 260/280 ratio and 260/230 ratio were referred to the purity of RNA samples. Total RNA isolates were kept at -80°C until the day of use.

2.4 DNAse I Treatment and cDNA Synthesis

RNA (1 µg) was treated with 1 µl DNAse I in a 10X reaction buffer according to the manufacturer's guidelines to remove any residual genomic DNA contamination in mRNA. DNAse I treatment was followed by first strand cDNA synthesis with oligodT primers by using Fermentas cDNA synthesis kit according to the manufacturer's guidelines.

2.5 RT-PCR and qRT-PCR Experiments

In a 30 µl reaction mixture, gene-specific primers were used for amplification of differentiation marker genes; intestinal alkaline phosphatase, hic-5 and villin. mRNA expression levels of inflammation-related genes TNF-α, IL1-β, COX-2, ICAM-1 and VCAM-1 were assessed by RT-PCR for comparison between control and treatment groups. Primers designed for each experiment are provided in Appendix A. Annealing temperatures, cycle numbers as well as primer and $MgCl_2$ concentrations were optimized prior to each different reaction.

In a 20 µl reaction mixture, qRT-PCR reactions were prepared with 2X Fast Start SYBR Green Mastermix (Roche, Mannheim), 2 µl of forward and reverse primers each, designed for ICAM-1 mRNA (Please see Appendix A for primer specificities) and 2 µl undiluted template cDNA. Unlike conventional RT-PCR reactions, housekeeping gene GAPDH was amplified in separate tubes not to lead to the confusion in detected fluorescent signal; relying on the interaction of SYBR Green with double-stranded amplification product. Moreover, by using serial dilutions of cDNA, standard curves were constructed for both ICAM-1 and GAPDH expression in HT29 cells for the calculation of Ct values. Pfaffl method was utilized for the analysis of three-independent replicate of results together with the technical replicates included for each reaction and data was represented as fold change (Pfaffl 2001).

2.6 Alkaline Phosphatase Activity Assay

Cellular protein extracts were obtained as explained in section 2.7 and alkaline phosphatase activity measurements were carried out by using p-nitrophenyl phosphate substrate liquid system (Sigma, USA). The ready-to-use substrate (200

µl) was added into each well of a 96-well-plate and 10 µl of total protein extract from HT29 cells was mixed into substrate by pipetting. Following 30 min incubation at 25ºC in the dark, absorbance readings were recorded at 480 nm. Specific enzyme activity was calculated after blank subtraction by dividing the absorbance values to the corresponding protein concentration.

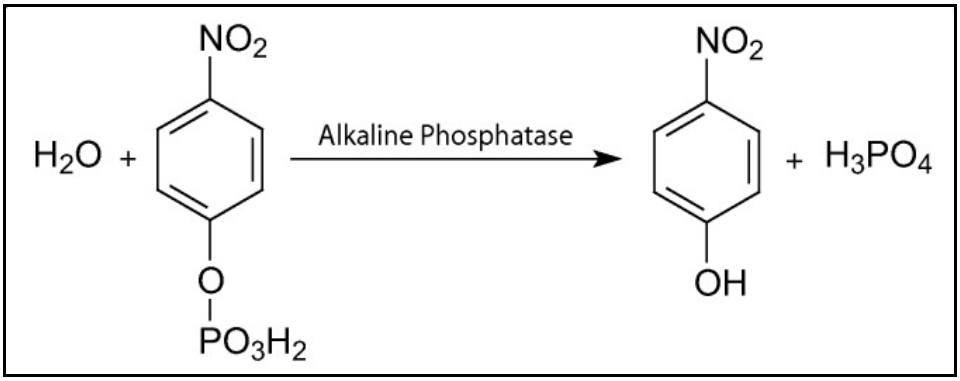

Figure 2. 1 Catalytic reaction by alkaline phosphatase leads pNPP substrate to develop p-nitrophenol (a soluble, yellow end-product).

2.7 NBT/BCIP Staining Assays

For this experiment, an assay solution composed of 0.4 mg/ml NBT (Sigma-Aldrich), 0.19 mg/ml BCIP (Sigma-Aldrich), 50 mM $MgSO_4$ was prepared in 100 mM Tris buffer at final pH 9.5, filtered through 0.45 µm Minisart filter and kept on ice. Cells grown in 6-well-plates were washed twice with TBS buffer pH 7.4. Fixation of cells was carried out in 70% molecular biology grade ethanol at RT for 10 min. Following two washing steps with TBS, staining was done with 500 µl of assay solution per well at RT for 2 hours. Excess solution was removed and the wells were washed three times with TBS buffer. Images of cells in TBS buffer were captured with an Olympus phase contrast microscope with a 10X objective

2.8 Protein Extraction from Cultured Cells

For protein isolations $3x10^5$ cells were seeded on 6-well-plates two days ahead of the treatment. Cells were treated with varying concentrations of sodium butyrate from 1 mM to 5 mM dissolved in cell culture grade PBS. Forty eight hours after treatment, total protein extraction was carried out from cell lysates by using M-PER Mammalian Protein Extraction Reagent (Pierce, USA) with protease inhibitors (Roche, Germany) according to the manufacturer's guidelines. For expression analysis of phosphorylated proteins phosphatase inhibitors were also included in the prepared lysis buffer. Protein concentration in the lysates was assayed by using Coomassie Plus Protein Assay Reagent (Thermo, USA) followed by reading the absorbances at 595 nm and calculations for concentration were done by using a standard curve constructed with BSA standards for that batch of reagent. Calibration curve used following each assay is provided in Appendix C.

2.9 Immunostaining Experiment on Coverslips

For immunostaining procedures $1x10^5$ cells were seeded on uncoated 18 mm round glass coverslips in 12-well plates and allowed to attach overnight. The cells were then treated with 3 mM sodium butyrate in refreshed culture media for 48 hours. Where indicated, cells were treated with 10 ng/ml TNF-α for 6 h or with 20 μM Bay 11-7085 for 3 h. Staining protocol for each sample and control group was started simultaneously at the end of 48 h treatment with sodium butyrate. First of all, culture media was removed and the cells were washed twice with PBS. Then, fresh 4% paraformaldehyde in PBS pH 7.4 was used for fixation of cells at RT for 10 minutes. Following fixation, the residual formaldehyde was removed with two washed with PBS and the cells were permeabilized with 0.3% Triton X-100. Blocking was carried out in 1% BSA solution and coverslips were incubated

overnight at 4ºC in specific primary antibody in 1% BSA solution. p65 rabbit polyclonal antibody (Santa Cruz) was used at a dilution of 1:100 whereas p50 rabbit polyclonal antibody (Santa Cruz) was used at a dilution of 1:200. Prior to the experiment, specificity of these antibodies were assessed by western blot analyses with HT29 protein lysates. For labeling the protein of interest at its corresponding subcellular localization, AlexaFluor488 conjugate of goat anti-rabbit antibody (Invitrogen, USA) was used at a dilution of 1:500 per sample. Nuclear staining was achieved by using propidium iodide (Sigma-Aldrich). 20X images were obtained with epifluorescent microscope (Leica DM 6000 B) by using appropriate filter cubes for both red and green channels.

2.10 Western Blot Analysis

Protein lysates were boiled in a reducing and denaturing sample loading buffer at 95°C for 6 minutes and loaded on a 4% stacking gel casted above a 10% or 12% SDS-PAGE gel for the separation of proteins. Electrophoresis was carried out under 100 V in Tris-Glycine buffer for 2-3 hours at room temperature. Vertically separated protein bands were transferred onto a pre-hydrated and equilibrated PVDF membrane in a sandwich cassette by wet-blot method in transfer buffer under 100 V for 1hour and 15 minutes at 4°C. Blotted membranes were blocked with 5% BSA in Tris-Buffered Saline containing 0.1% Tween-20 (TBS-T) for 1h at room temperature or for overnight at 4 ºC. Dilutions of primary antibody at 1:500-1:1000 in blocking agent were used for probing the protein of interest at 4ºC overnight. On the following day, after three sequential washes for 10 minutes each in TBS-T buffer, the membrane was incubated at room temperature with constant shaking in a 1:2000 dilution of the appropriate HRP-conjugated secondary antibody for 1 h. Unbound, excess antibody was removed by three washing steps with TBS-T and then 1:1 mixture of luminal:peroxide ECL substrate was applied on the probed membrane for a 1 min at room temperature. Substantial chemiluminescent reaction was detected by exposure of membranes to

the X-ray film (Kodak) for 5 to 120 seconds in a dark room. Kodak X-Ray processor was used for fixing and developing the signal on the X-ray film.

2.11 Chromatin Immunoprecipitation Experiments

$2.5x10^6$ cells were seeded on 100 mm cell culture dishes and grown to 70% confluency. Then, cells were either left untreated or treated with 3 mM NaBt for 48 h. On the first day of experiment, formaldehyde was added into fresh culture media at 0.75% final concentration and in order to crosslink DNA-binding proteins to chromatin, adherent cells were incubated with this medium for 7 min with constant agitation at room temperature. Glycine was used at 125 mM final concentration for quenching the formaldehyde and to stop further crosslinking reaction. Crosslinked cells were scraped into ice-cold cell culture-grade PBS after the removal of residual chemicals and pelleted. The cell pellet was snap-frozen in liquid nitrogen and redissolved in Buffer A to disrupt the cellular membranes. After incubation on ice for 20 min, cell nuclei was separated from total lysate by centrifugation and nuclear enriched cell lysate was obtained after resuspension in Buffer B. Chromatin was fragmented by using a probe sonicator at 20% of the maximum power for 7 cycles of 30 s sonication with sequential incubations on ice for another 30 sec. For fragment size analysis, 3 µl of sonicated lysate was electrophoresed in 1.5% agarose gel. For each experiment, 75 µl from the total cell lysate was spared as input control and rest of the lysate was snap-frozen in liquid nitrogen. DNA concentration of cell lysate was assessed following a phenol-chlorofom isolation protocol of the input sample. Before starting immunoprecipitation, protein A/G beads were prepared by blocking in BSA and calf-thymus DNA. According to the concentration calculations, equal amount of DNA sample was aliquoted into microcentrifuge tubes and diluted with Buffer C. 5-10µg of antibody was added for an overnight incubation of samples at 4ºC with constant shaking. Then, 15-20 µl blocked bead was added on the following day and incubated for 1-2 hours at 4 ºC with constant rotation. Antibody-bound beads

were pelleted at 3000 rpm for 5 min. Following two low-salt buffer washes and one high-salt buffer wash, chromatin fragments were eluted from beads with 1% SDS buffer. Following elution, RNAse A and proteinase K digestions were carried out and reverse-crosslinking was achieved by overnight incubation at 60 °C with constant rotation at approximately 180-200 rpm. Phenol-chloroform isolation was utilized for purifying DNA. Precipitated DNA samples were used as template in RT-PCR for analyzing transcription factor recruitment on promoter regions of gene of interest. Primer sequences are provided in Appendix D.

2.12 Phenol-Chloroform Extraction of DNA

Chloroform : Isoamylalcohol 24:1 solution and pH 7.0 equilibrated, non-stabilized phenol were purchased from AppliChem, Germany. 1:1 mixture of these two solutions was prepared in a fume hood freshly just prior to use. For an approximately 500 µl RNAse A and proteinase K treated lysate, 500 µl of this mixture was added and mixed. Organic phase, interphase and aqueous phase were separated after centrifugation at 13000 rpm for 10 minutes at 4 ºC. This step was repeated to get rid of any protein contamination as much as possible and to increase nucleic acid yield. Then, the aqueous phase was washed twice with chloroform and collected after centrifugation at 13000 rpm to remove any phenol contamination. Upon collecting the final aqueous phase, 1:10 volume of 3 M sodium acetate and 2X volume of molecular biology grade absolute ethanol was added and samples were left at -20 ºC up to one day for efficient DNA precipitation. On the following day, DNA was pelleted at 13000 rpm at 4 ºC for 30 min. Following a 70% ethanol wash, the DNA pellet was precipitated again for 10 min, and then allowed to dry at RT. After all the ethanol was evaporated, the pellet was resuspended in MilliQ water. DNA concentration was measured by Nanodrop, 260/280 and 260/230 absorbance ratios were utilized for the assessment of the purity.

2.13 Statistical Analyses

For each experiment, at least three technical replicates were carried out for each of three biological replicates. Data analysis and graphing were carried out using GraphPad Prism (La Jolla, California). Statistical significance between groups was carried out using Students t-test and was considered to be significant at the level of $p<0.05$.

CHAPTER 3

RESULTS AND DISCUSSION

HT29 are tumorigenic epithelial cells that are derived from colorectal adenocarcinoma with adherent growth properties. They have upregulated myc, ras, fos, and mutated p53. In addition to some other cell lines such as Caco-2, HT29 cells have been used as a model of colon differentiation for years. (Cohen et al. 1999) In this study effect of NaBt-induced differentiation on inflammatory pathways was investigated in an in vitro model using HT29 to understand the cellular mechanism of the anti-tumor effect exerted by this SCFA.

3.1 Characterization of Differentiation in Sodium Butyrate Treated HT29 Cells

For the assessment of differentiation in NaBt treated HT29 cells, expression of several well-known differentiation markers were assayed (Figure 3.1). Intestinal alkaline phosphatase (IAP), a peripheral membrane protein with GPI anchor, is a brush-border enzyme and a well known differentiation marker for colonocytes (Chang et al. 2008). This gene showed a drastic increase in expression upon treatment with 3 mM NaBt. Another marker Hic-5, a paxillin homolog protein that is involved in focal adhesion complex and also acts as a nuclear receptor coactivator that has been investigated to have roles in senescence, differentiation and apoptosis (Drori et al. 2005). Hic-5 was also shown to be upregulated

drastically after 3 mM NaBt treatment. In addition to that, Villin-1, a protein involved in the reorganization of actin filaments in the microvilli in the apical side of the colonic epithelia (Chang et al. 2008) was also upregulated in response to NaBt treatment. To further confirm the differentiation status of cells, alkaline phosphatase activity assay was also carried out as explained in Section 2.5 according to the manufacturer's instructions and the highest fold change in the activity of alkaline phosphatase was observed in response 3 mM treatment as well (Figure 3.1).

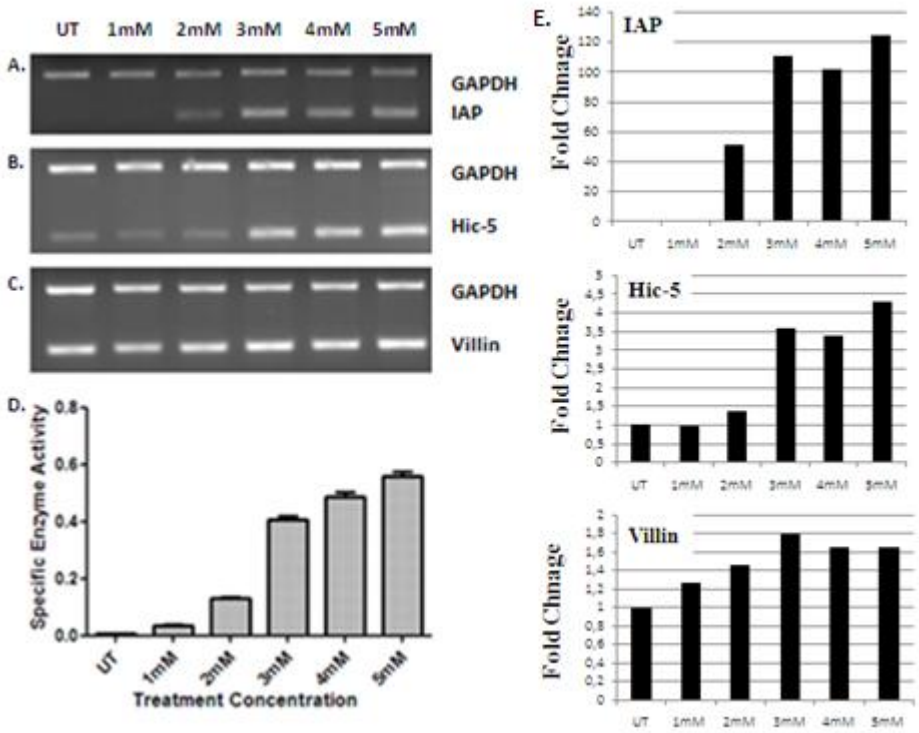

Figure 3.1 Analysis of differentiation status in 1-5mM sodium butyrate treated HT29 cells. A: mRNA expression level of intestinal alkaline phosphatase, B: mRNA expression level of Hic-5, C: mRNA expression level of Villin-1 in NaBt-treated HT29 cells. D: Measurement of alkaline phosphatase activity in 1-5 mM NaBt-treated HT29 cells. E: Densitometric analysis of IAP, Hic-5 and Villin RT-PCR results presented as fold change according to untreated control sample.

Moreover, the NBT/BCIP staining assay, an indicator of *in vivo* alkaline phosphatase activity, provided further evidence for the differentiation of HT29 cells treated with 3mM NaBt (Figure 3.2). In this assay, BCIP provides the substrate for IAP and NBT enhances the staining by forming insoluble precipitates together with IAP-catalyzed, soluble BCIP product. As can be seen in Figure 3.2, besides the brown staining -the outcome of IAP activity- it is also possible to observe general differences in morphology of HT29 cells that are exposed to varying concentrations of NaBt. Moreover, NaBt could also diminish the proliferation rate of cells as shown by the empty patches in the treated wells whereas untreated cells have covered all over the surface within that 48 hours of treatment.

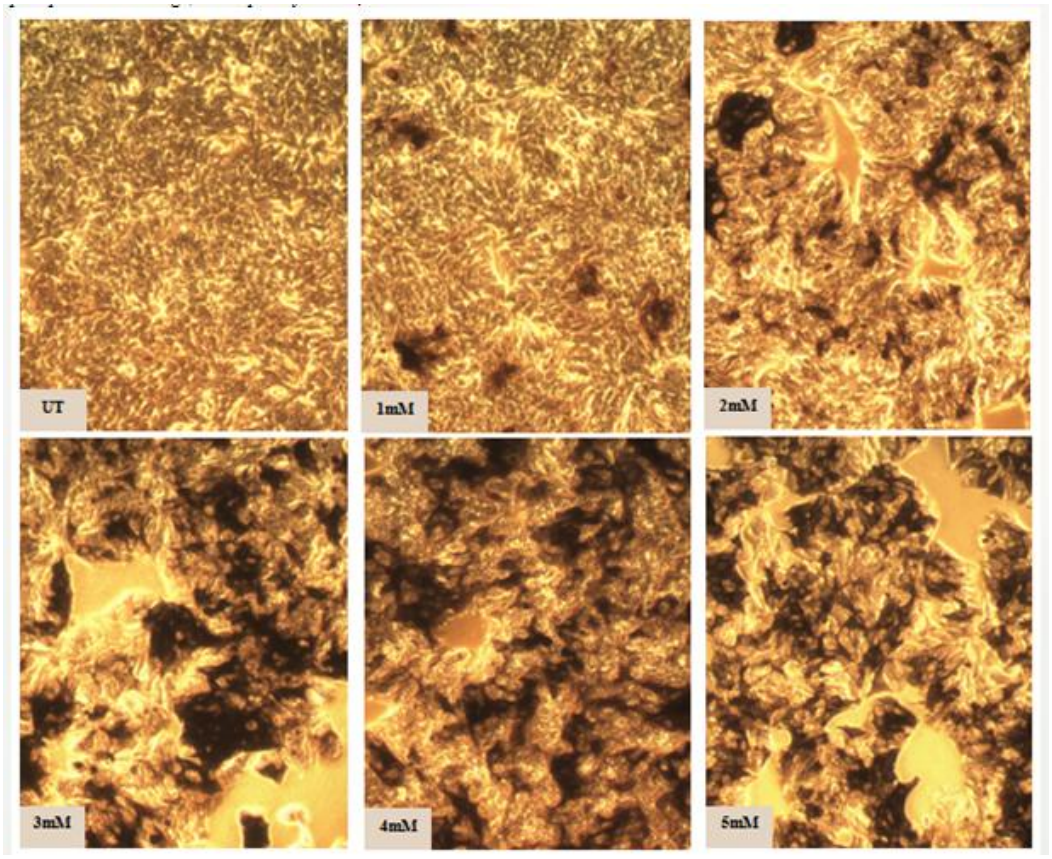

Figure 3.2 Alkaline phosphatase staining assay. Phase contrast images of HT29 cells in TBS are obtained at 10X magnification with 1024 x 768 resolution, indicating alkaline phosphatase staining. As indicated for each frame, from upper left to the bottom right, images belong to untreated or 1mM, 2mM, 3mM, 4mM and 5mM NaBt-treated HT29 cells respectively.

3.2 Investigation of Subcellular Localization of NF-kappaB Subunits

Our group has recently shown that spontaneous differentiation in colon cells, that is induced by growing cells in culture flasks after post-confluency, lead to the inhibition of nuclear factor kappa B (NF-kappaB), an important transcription factor that plays a role in many cellular functions related with proliferation, differentiation, apoptosis as well as inflammation (Astarci, et al, 2012). In order to determine whether chemically induced differentiation through the treatment of cells with NaBt could also lead to a similar inhibition of NF-kappaB, we have investigated NF-kappaB activity in NaBt treated cells. This is especially relevant in colorectal cancer, a cancer that can be promoted by inflammation. We therefore aimed to study the effect of NaBt-induced differentiation on inflammatory pathways in HT29 adenocarcinoma model and whether NF-kappaB is a key regulator that participates in the crosstalk of these two cellular phenomena, that are, inflammation and differentiation.

The first approach was to investigate the subcellular localization of the NF-kB subunits p50 and p65. Since the NF-kappaB transcription factor subunits are active upon their localization into the nucleus, we have determined the localization of p50 and p65 in response to NaBt treatment. For this purpose, an immunostaining experiment was carried out using HT29 cells seeded on uncoated- glass round coverslips (18mm) as explained in Section 2.8. Staining was done for both p50 and p65 subunits of NF-kappaB. In addition to untreated and NaBt treated HT29 cells, two further control groups were included. One of those control groups was HT-29 cells treated with Bay 11-7085 which inhibits NF-kappaB via the irreversible inhibition of TNF-α-stimulated IκBα phosphorylation with an IC_{50} value of approximately 10 μM. The second control group consisted of cells treated with recombinant TNF-α protein as an inducer of NF-kappaB activity. Therefore, the effect of NaBt on NF-kappaB activity could be compared to well-established activator and inhibitor of the

transcription factor. Three biological replicates of the experiment were conducted and images were captured from at least five randomly chosen areas of each cover slip. Representative images for p50 immunostaining are provided in Figure 3.3, and for p65 immunostaining in Figure.3.4.

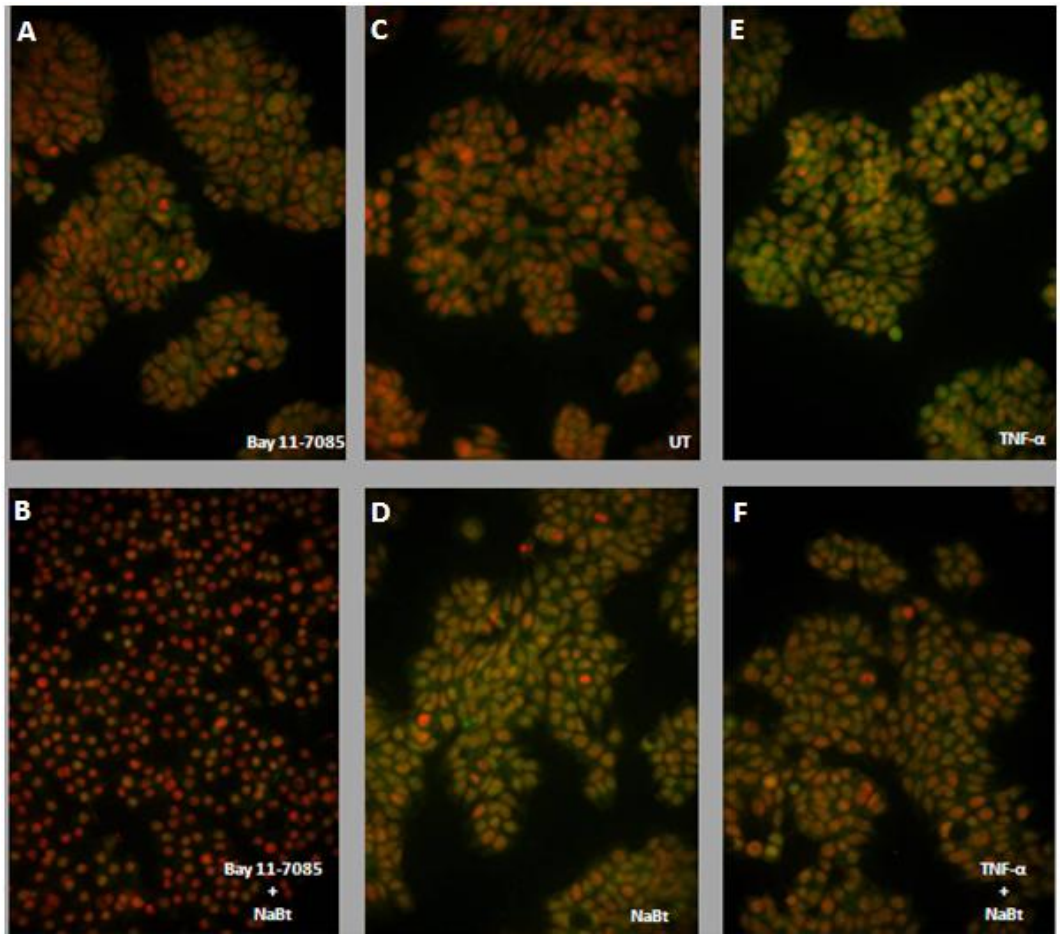

Figure 3.3 Subcellular localization of p50 in response to NaBt. Images are obtained under 20X magnification with Leica DM 6000 B epifluorescent microscope. Green channel signal indicating Alexa Fluor 488-labelled p50 and red channel signal indicating propidium iodide stained nuclei are merged with Image J software. A: Bay 11-7085 treated, B: Bay 11-7085 + NaBt treated , C: Untreated, D: NaBt treated, E: TNF-α treated, F: TNF-α + NaBt treated HT29 cells.

Secondary antibody raised against primary antibody of the protein of interest was an AlexaFluor488 conjugate, thus localization of either p50 or p65 was marked by green fluorescent signal in the images. As illustrated in the middle panels in Figure 3.3 intense nuclear accumulation of p50 was observed in response to NaBt treatment in HT29 cells. The p50 subunit of NF-kappaB may exist either as a homodimer or heterodimer complex inside the nucleus. Although there is evidence that p50 homodimer may have a transactivating role upon interaction with some tertiary interactors such as Bcl-3 or DNA-PK, it is most commonly associated with a repressor effect on transcription (Ju et al. 2010, Ghosh 2007). On the other hand, if it forms a heterodimer with p65, it leads to transactivation and transcriptional upregulation of target genes. Although there is possibility that dense nuclear staining of p50 subunit might be representing the presence of homodimer inside the nucleus rather than a heterodimer, by comparing the upper and lower middle panels, only effect of NaBt on NF-kappaB subunit localization can be understood. As a comparison, the upper left panel shows inhibited NF-kappaB pathway with Bay11-7085 whereas the upper right panel shows the activated NF-kappaB pathway with TNF-α. While the p50 localization appeared to be similar in untreated (UT) and Bay 11-7085 treated cells, there is an obvious difference when cells were treated with Bay 11-7085 together with NaBt, indicating the possibility of a synergistic inhibitory effect on NF-kB activity. On the other hand, we do not observe such a drastic difference for TNF-α treated samples either in the absence or presence of NaBt. Moreover, when we compare NaBt treated sample with TNF-α + NaBt treated sample, we can see that p50 nuclear localization in nucleus is less in TNF-α + NaBt treatment. This may provide, at least to an extent, support for our hypothesis regarding NF-kB activity in NaBt treated cells. We have hypothesized that the p50 subunits translocate to the nucleus in a homodimer complex which may lead to a reduction in NF-kB activity. In the presence of TNF-α, an activator of the pathway, p50 would be expected to translocate to the nucleus in a heterodimer complex with p65 instead of forming homodimer and occupying kappaB elements on DNA. Therefore, less green signal would be expected to be observed in the nucleus in TNF-α + NaBt treated sample in comparison to only NaBt treated sample, as can be seen in

Figure 3.3. However, in order to substantiate this hypothesis of the nuclear translocation of inhibitory homodimeric p50 subunits, further detailed experiments are needed (Please see the section on future studies).

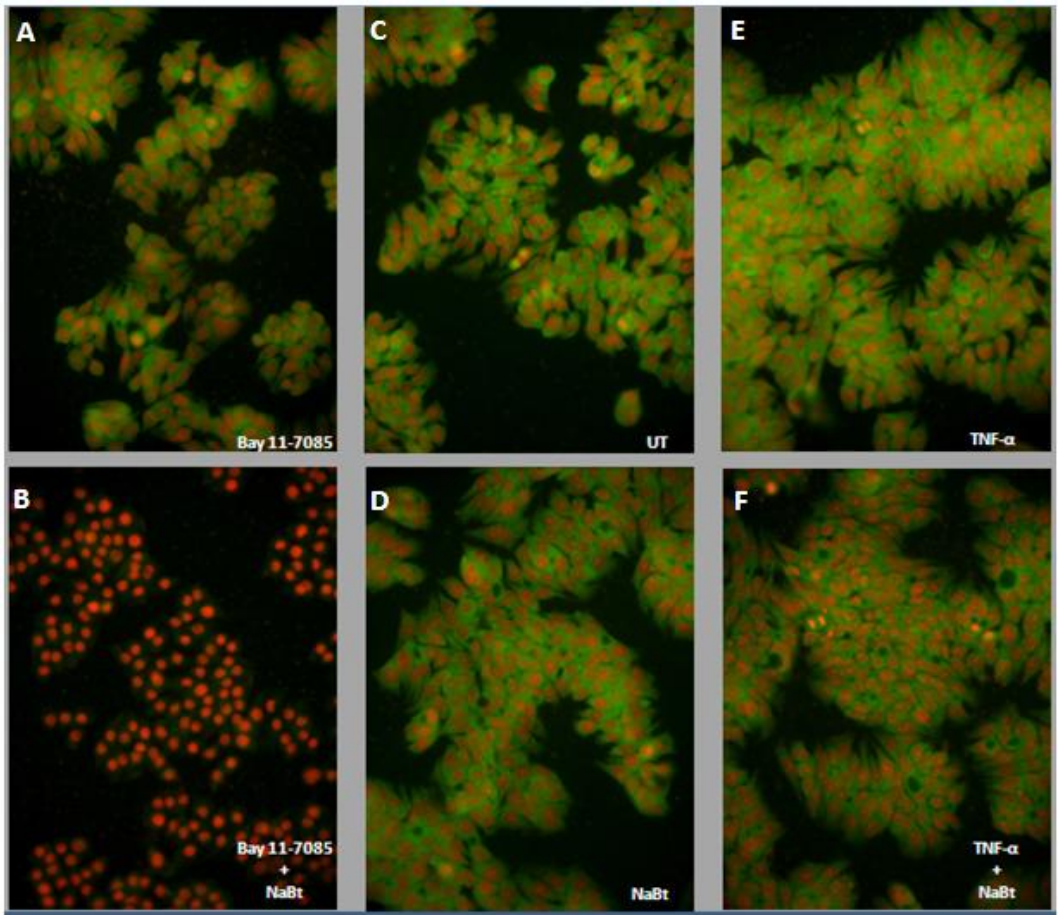

Figure.3.4 Subcellular localization of p65 in response to NaBt. Images are obtained under 20X magnification with Leica DM 6000 B epifluorescent microscope. Green channel signal indicating Alexa Fluor 488-labelled p65 and red channel signal indicating propidium iodide stained nuclei are merged with Image J software. A: Bay 11-7085 treated, B: Bay 11-7085 + NaBt treated , C: Untreated, D: NaBt treated, E: TNF-α treated, F: TNF-α + NaBt treated HT29 cells.

Immunostaining to determine subcellular localization of p65 was also carried out. Similar to p50, Bay 11-7085 + NaBt treatment showed a complete loss of staining of p65, whereas p65 localization was not dramatically affected in the other treatment groups. This indicates that NaBt preferentially enhanced the nuclear localization of p50, with little or no effect on the localization of p65. As discussed above, since nuclear localization of both p65 and p50 is necessary for the canonical NF-kB pathway to be activated, the selective enhancement of p50 localization to the nucleus further indicates the possibility of the formation of p50 homodimers.

Bay 11-7085 and some other inhibitors are being utilized to represent a model for repressed NF-kappaB activity in research with several purposes. As summarized in a review article, treatment of cells with certain NF-kappaB inhibitors such as Bay 11-7085, Bay 11-7082 or proteasomal inhibitors together with chemotherapeutic, cytotoxic or anti-proliferative drugs lead to sensitization of tumor cells to the drug of interest. It was mentioned that cytotoxic drug resistance developing in cancer cells due to the presence of a constitutively active NF-kappaB pathway might be overcome by cotreatment with an NF-kappaB inhibitor (Nakanishi and Toi 2005). In correlation with these suggested mechanisms we have also found the most drastic anti-tumor response from cells upon cotreatment with NaBt and Bay 11-7085.

3.3 Effect of Sodium Butyrate on NF-kappaB Target Genes

For further investigation of NF-kappaB activity, mRNA level of some of the NF-kappaB target genes were analyzed by RT-PCR. For this purpose, HT29 cells were treated with NaBt for 48 hours and total RNA was purified by using Qiagen RNeasy Minikit, quantified with the Nanodrop and cDNA synthesis was carried out. Finally, amplified cDNA products were analyzed on agarose gel following RT-PCR. For each assay three independent biological replicates were carried out and the PCR products were electrophoresed on the same gel. As can be seen in Figure 3.5 and Figure.3.6, IL1-β and TNF-α mRNA expressions were enhanced in response to NaBt treatment. Both TNF-α and IL1-β are cytokines that are expressed and released by cells in an inflammatory response (Janeway et al. 2004). Moreover, both have NF-kB binding sites in their promoter regions. There is ample evidence in literature on the anti-inflammatory effect of sodium butyrate (Segain et al. 2000, Wong et al. 2006) making the upregulation of these cytokines contradictory, as both TNF-α and IL1-β expression would indicate the cell's response to inflammation. However, there are two possible explanations for this.

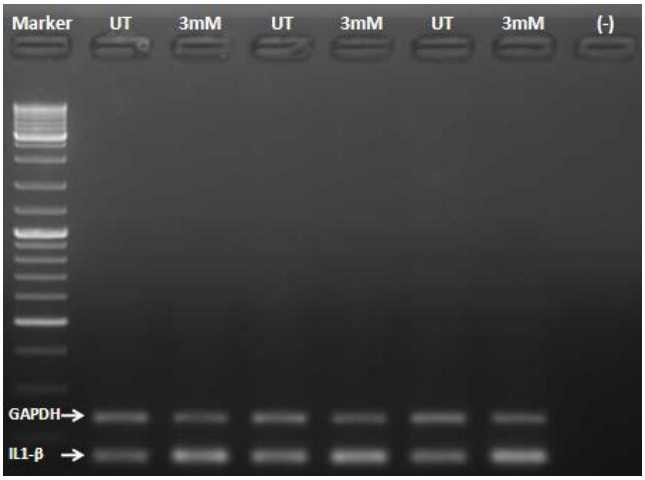

Figure 3.5 IL1-β RT-PCR for three independent replicates of untreated versus 3mM NaBt treated HT29 RNA samples.

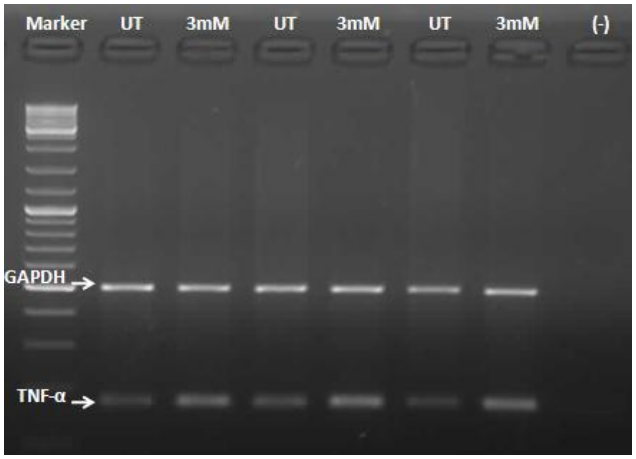

Figure 3.6 TNF-α RT-PCR for three independent replicates of untreated versus 3mM NaBt treated HT29 RNA samples.

First, our *in vitro* model system of differentiation is with a cancer cell line, which, although mimicking the process of cellular differentiation, nonetheless, has signaling pathways that may be unlike normal cells (Simon-Assman et al. 2007) Neoplastic cells are well-known for their ability to adapt to different microenvironments, to evade certain mechanisms reducing their proliferation which would potentially affect normal cells. Multidrug resistance can be considered as one of the most well-known mechanism as an example (Juliano and Ling 1976). In our case, since we are inducing differentiation chemically by exposing aggressively proliferating tumor cells to NaBt, HT29 cells might be trying to avoid differentiation and reduction in proliferation by activating certain survival mechanisms. Therefore, upregulation of TNF-α and IL1-β might be a survival signal sent to neutrophils and other phagocytic cells that are able to provide them growth stimulating factors.

Secondly, in adenocarcinomas (the tumor type from which HT29 cells originated) there is also specific evidence of the upregulation of TNF-α and IL1-β as a process activation of an adaptive immune response against cancer (Morgan et al. 2004). In addition to this, since SCFAs are bacterial metabolites, they may help to

activate the immune system much faster in case of an infection by helping to reach the threshold level for induction of response much easily. Combining these evidences together, it might be hypothesized that although there is an upregulation of pro-inflammatory factors in the presence of NaBt, the outcome might be activation of the adaptive immune response against the tumor.

Another NF-kappaB target gene that plays a role in immune responses is ICAM-1; the interaction partner of LFA-1 as explained in the section 1.3.3. Expression level of ICAM-1 was investigated at mRNA and protein level upon NaBt treatment (Figure 3.7). An alteration in the mRNA transcript level of ICAM-1 in response to NaBt was not detectable with conventional RT-PCR. However, by utilizing a much sensitive method, with quantitative RT-PCR, we have observed nearly two fold increase that was beyond the sensitivity of an ethidium bromide dependent-detection method following an agarose gel electrophoresis. In addition to that, a significant increase in protein expression was observed in all three independent replicate of experiments. ICAM-1 expression is shown to be deregulated in neoplastic cells. Colorectal adenocarcinoma cells also express ICAM-1. In a study, it was shown that ICAM-1 has a role in leukocyte-epithelial cell interaction in colon adenocarcinoma, which might be considered as a part of the immunosurveillance system (Kelly et al. 1992).

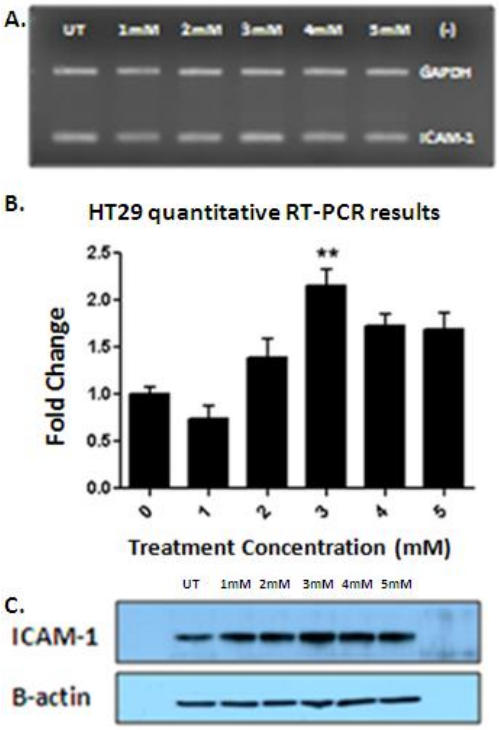

Figure 3.7 A: RT-PCR, B: qRT-PCR and C: western blot analysis of ICAM-1 from three independent replicates of untreated versus 1-5mM NaBt-treated HT29 cell extracts. Reaction efficiency in quantitative RT-PCR for ICAM-1 reaction is 1.038, for GAPDH reaction is 0,8027. Normalized and analyzed data is represented as fold change according to the untreated sample.

Similarly, another immunoglobulin superfamily member, VCAM-1 was also investigated in the scope of this study at both mRNA and protein level. *In vivo*, VCAM-1 is known to undergo interaction with VLA-4, also called as integrin α4β1. Similar to LFA-1 partner of ICAM-1, VLA-4 is also a heterodimeric integrin protein expressed on leukocyte plasma membranes (Janeway et al. 2004). As shown in Figure 3.8, VCAM-1 has also shown substantial increase at protein level as well as mRNA level.

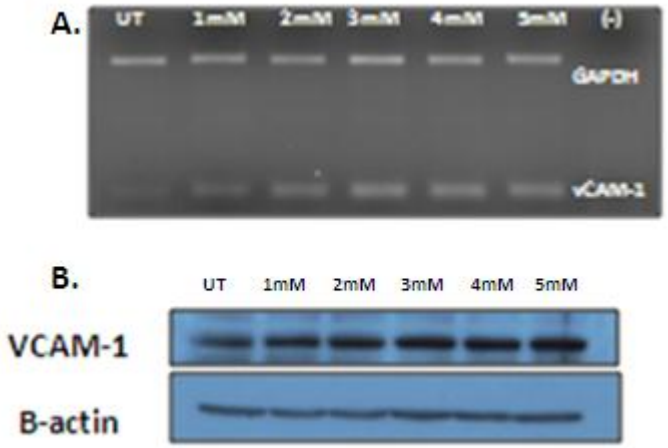

Figure.3. 8 A: RT-PCR and B: western blot analysis of VCAM-1 from three independent replicates of untreated versus 1-5mM NaBt treated HT29 cell extracts.

Increased ICAM-1 and VCAM-1 expression in sodium butyrate induced differentiation might be a further proof of an evoked immunosurveillance system against these tumor cells. Therefore, NaBt treatment could indeed be a transition state that promotes tumor cell recognition by the immune system, rather than a state of a terminal differentiation into normal colonocytes.

Yet another NF-kB target gene that is involved in the process of inflammation is COX-2. COX-2 codes for an enzyme that catalyzes the conversion of arachidonic acid to prostaglandin endoperoxidase H2 (PGE-2). Proliferative ability of tumor cells is shown to be enhanced by COX-2 overexpression as well as prostaglandin biosynthesis. On the other hand, prostaglandins, especially PGE-2 are also well-known for their suppressive effects on the immune system. Previously, an increased level of PGE-2 in plasma was attributed to;

- Decreased levels of anti-tumor factor (IFN-γ, TNF-α) secretion by T-cells,
- Decreased secretion of dendritic cell-stimulatory molecules,

* Impaired phagocytic activity of dendritic cells,
* Failure to undergo dendritic cell maturation.

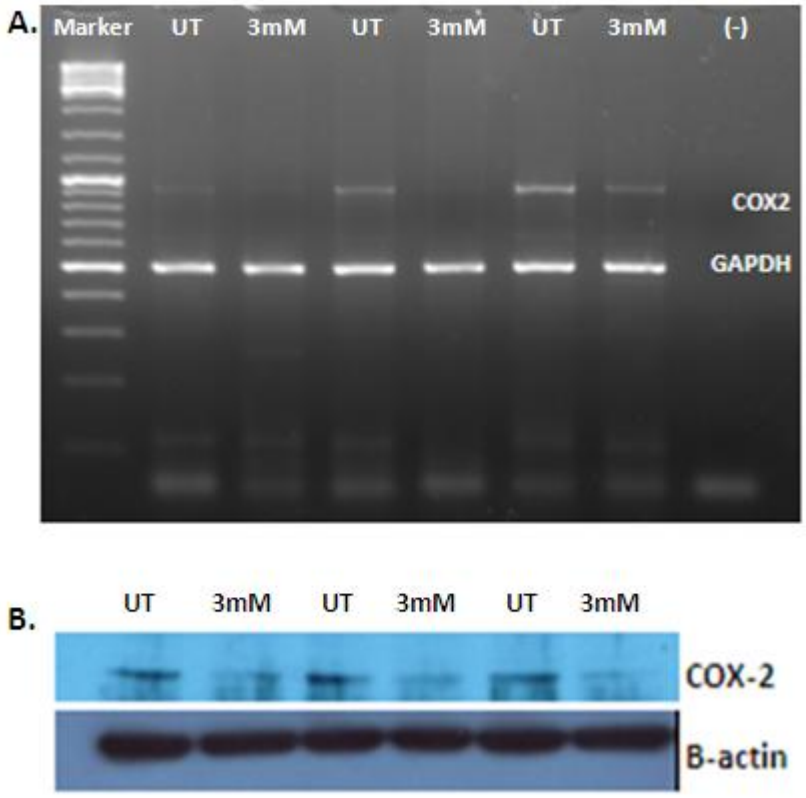

Figure.3.9 A: RT-PCR and B: western blot analysis of COX-2 from three independent replicates of untreated versus 3mM NaBt treated HT29 cell extracts.

Noting that dendritic cells and T-cells are the most prominent components of immunosurveillance system, increased PGE-2 synthesis in tumor microenvironment has the great potential to protect tumor cells from a potent immune attack (Harris 2007).

In our study, COX-2 expression in response to NaBt treatment was analyzed by RT-PCR and Western blots (Figure.3.9). A significant reduction in COX-2 gene expression was observed in mRNA level. Moreover, COX-2 was downregulated

at protein level as well. Since, COX-2 expression in colorectal carcinoma is directly associated with neoplastic progression (Morgan et al. 2004, Harris 2007), this data may imply that NaBt may not only activate immune surveillance against cancer cells, but also directly prevent neoplastic progression of tumor cells. Moreover, a downregulation in COX-2 expression also proves that NaBt does not solely lead to global enhancement in gene expression due to its histone deacetylase activity; rather, this is a specific chemopreventive function of NaBt.

3.4 Investigation of p50/p65 Recruitment on Promoter Regions of NF-kappaB-dependent Inflammatory Markers

Chromatin immunoprecipitation assay was utilized to be able to investigate the recruitment of p50 and p65 subunits of NF-kappaB on promoter regions of target genes. Prior to carrying out the experiment for the transcription factor-promoter interaction of interest, a set of optimization steps were conducted (Please see Appendix A). Upon completing the first set of optimizations, assay protocol was followed for immunoprecipitating distal kappaB sites on ICAM-1 promoter region with p50 and p65 antibodies. In Figure 3.10 a representative image from our preliminary results is given.

HT29 cells treated with NaBt or with the vehicle were crosslinked and sheared by probe sonication. The chromatin was then immunoprecipitated with p50 and p65 antibodies bound to protein A/G beads as described in Section 2.11. Amplification of the immunoprecipitated chromatin with primers designed to amplify NF-kappaB consensus sequences in the promoter of the ICAM-1 gene showed that NaBt treatment resulted in lower enrichment of p65 whereas p50 recruitment was observed to increase in the promoter of ICAM-1 (Figure 3.10). In the experiment, input control is referred to the total amount of chromatin purified from untreated

control and treatment groups, whereas the IgG isotype control refers to the specific interaction between antibody and DNA. The beads only control groups refer to the non-specific association between chromatin and beads. As can be seen in Figure 3.10, minimum signal was obtained from the IgG and beads only control experiments, further attesting to the specific signal obtained from chromatin immunoprecipitated with the p50 and p65 antibodies.

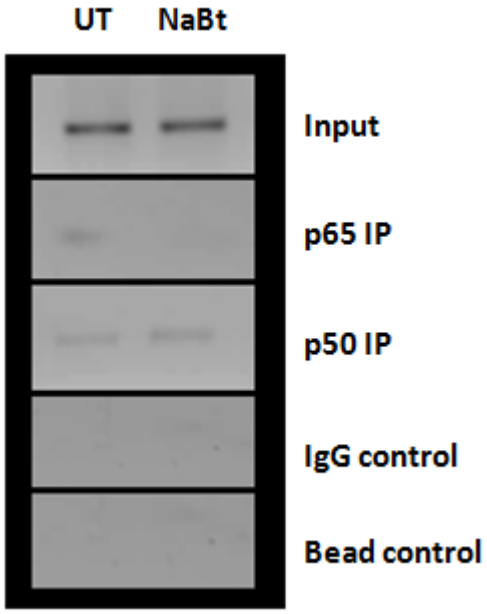

Figure 3.10 ChIP-PCR for ICAM-1 promoter upon p50 and p65 IP. UT: untreated HT29 chromatin samples, NaBt: sodium butyrate-treated HT29 chromatin samples. Amplification product is distal κB site on ICAM-1 promoter. Immunoprecipitated samples with p65, p50 and IgG antibodies together with beads only control and input chromatin for UT and NaBt samples served as template for PCR reaction.

Although enhanced recruitment of p50 and reduced recruitment of p65 was indicating the parallel results with the immunostaining experiments, the data we have obtained does not correlate with the increased transcript level of ICAM-1 that we have observed in response to NaBt treatment. These data suggest that there might be other transcription regulators on the ICAM-1 promoter having a

more potent effect on gene transcription than NF-kappaB. This was also explained in a recent article by our group that ICAM-1 gene has CEBP-binding regions in its promoter as well (Astarci et al. 2012). Therefore, further studies will be carried out on inflammation-related genes to investigate the NF-kappaB link in NaBt induced inflammatory response.

CHAPTER 4

CONCLUSIONS

In this study, we aimed to investigate the link between the expression of inflammatory markers and the induction of differentiation as a result of treatment of HT29 cells with sodium butyrate (NaBt). For this purpose;

I. We have confirmed the induction of differentiation in HT29 cells after treatment with varying concentrations of NaBt.
   - An increase in the expression of differentiation markers IAP, Hic-5 and Villin-1 was observed when cells were treated with increasing concentrations of NaBt.
   - Quantitative and qualitative analyses of IAP activity was carried out with a colorimetric enzyme activity assay and NBT/BCIP staining respectively. Both assays showed the presence of active IAP, as well as a dose-dependent increase in the activity in response to NaBt treatment. This increase in IAP activity was seen in the HT29 cells with treatments of up to 3mM, after which there was a decrease. At 4mM and 5mM concentrations, cell numbers decreased considerably as the cells underwent apoptosis.

II. As the primary inflammation-associated transcription factor, the activity of NF-kappaB pathway was then determined in the presence of NaBt induced differentiation.

* Subcellular localization of canonical NF-kappaB pathway components was determined by immunofluorescent staining of p65 (Rel A) and p50 (NF-kappaB1). p50 was found to be primarily translocated to the nucleus in the NaBt treated cells, however, p65 localization did not show a drastic change in response to the treatment. Experimental controls, in which NF-kappaB activity was either blocked with Bay 11-7085 or induced with TNF-α in untreated versus NaBt treated samples, provided additional information on the implications of the effect of NaBt on NF-kappaB activity. Treatment of the cells with the NF-kappaB inhibitor along with NaBt, resulted in a complete abrogation of signal from both p50 and p65 proteins, suggesting a synergistic role of NaBt with the NF-kappaB blocker. On the other hand, treatment with NF-kappaB inducer did not show a drastic increase in nuclear translocation of these proteins; either alone or in the presence of NaBt. These data hinted towards an inhibitory role of NaBt in the NF-kappaB pathway.
* For further investigation of NF-kappaB activity, target gene expression of this transcription factor was evaluated. Interestingly, both of the inflammatory markers IL1-β and TNF-α were found to be upregulated in response to NaBt treatment. In addition to that, expression level of inflammation related-adhesion molecules ICAM-1 and VCAM-1 were also found to be upregulated.
* Results obtained up to this point, pointed towards an inflammatory response upon treatment with NaBt; which was contrary to the ample amount of published data on anti-inflammatory effects of sodium butyrate. (Segain et al. 2000, Wong et al. 2006) Considering the fact that NaBt also acts as an inhibitor of histone deacetylases (HDAC), which therefore allows the histones to remain acetylated, the chromatin relaxed and thereby lead to approximately >10% increased transcription (Glaser et al. 2003,

Peart et al. 2005), the increase in expression of the inflammatory markers could be attributed towards a global increase in gene expression. However, we have also observed that COX-2, a critical enzyme for an inflammatory response, was downregulated in response to sodium butyrate at both mRNA and protein levels. COX-2 expression in colorectal cancer has previously been associated with neoplastic progression (Morgan et al. 2004). Therefore, this inhibition could be an indication of reversal from the malignant phenotype.

* To be able to determine the role of NF-kappaB activity on alterations in inflammatory-marker gene transcription in response to NaBt treatment, chromatin immunoprecipitation protocol was established for HT29 cells and preliminary results after a set of optimizations indicated decresed p65 recruitment in the presence of NaBt whereas p50 was observed to be enriched in distal kappaB sites on ICAM-1 promoter region.

Based on the data we have obtained, we propose that NaBt might be switching on an immunosurveillance system in colorectal cancer cell lines by potentially inducing an innate or adaptive tumor-directed immune response. Upregulation of the expression of the cytokines IL1-β and TNF-α, as well as the upregulation of leukocyte integrin-binding proteins ICAM-1 and VCAM-1 could consequently promote leukocyte migration to the tumor site. Moreover, COX-2 downregulation, which may lead to reduced levels of PGE-2, has previously shown to upregulate anti-tumor factors secreted by T-cells such as IFN-γ, TNF-α, IL-2, IL-12, etc (Harris 2007). However, further experiments with appropriate controls are necessary to prove this hypothesis (please see the section on future studies below). In addition, consistent with our immunostaining results, p50 recruitment on distal kappaB sites on ICAM-1 promoter was found to be enhanced ollowing NaBt

treatment, whereas p65 recruitment was observed to be decreased. Although our results on ICAM-1 transcript level in response to NaBt seems to be contradicting with the inferences made on repressed NF-kappaB function via p50 homodimers, ICAM-1 promoter is shown to be regulated by several other transcription factors as well. To illustrate, in a recent article published by our group, CEBPβ was found to be an important regulator of gene transcription for ICAM-1 . (Astarci et al. 2012).

The effect of HDAC inhibitors on tumor and immune cells has recently been reviewed by Leggatt et al. Here, the authors have argued that HDAC inhibitors may suppress inflammatory signals in cellular components of immune system, while at the same time it enhances the inflammatory signals in tumor cells. Thus, systemic HDAC inhibitor-mediated tumor therapy is very likely to fail due to this bidirectional effect on immune cells and tumor cells (Leggatt and Gabrielli 2012). However, Khan et al. have proposed that ex-vivo treatment of tumor cells with HDAC inhibitors and reinjection to the patient can be a promising method to bypass the effect of HDAC inhibitors on immune cells (Khan, Magner and Tomasi 2007, Khan, Gregorie and Tomasi 2008).

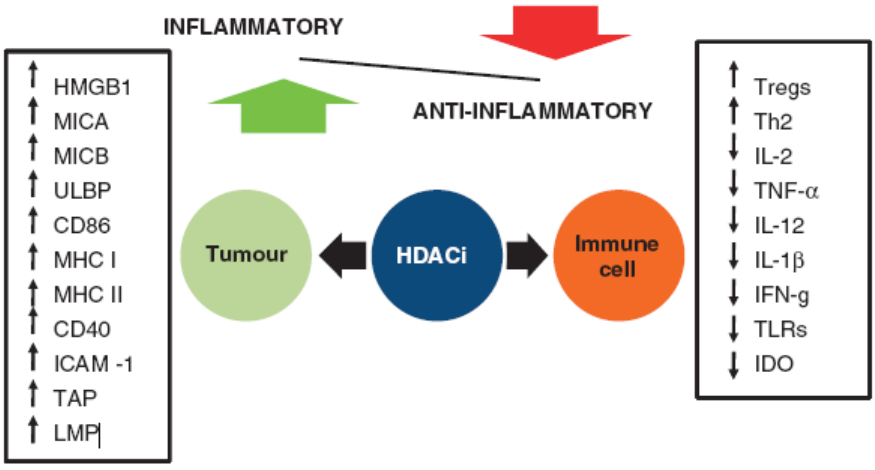

Figure 4. 1 Bidirectional pro-inflammatory and anti-inflammatory effects of HDACIs on different cellular targets (Leggatt and Gabrielli 2012).

Furthermore, HDAC inhibitor-mediated anti-tumor response may even potentially prevent the recurrence of secondary tumor growth; as adaptive immune response evoked against cancer cells by T-cells and B-cells may play role in construction of an immune memory (Leggatt and Gabrielli 2012).

Collectively, HDAC inhibitor-mediated cancer therapy may have the future potential to be used in monotherapeutic strategies or in combination therapies against cancer treatment, promising the prevention of tumor-recurrences and metastasis.

CHAPTER 5

FUTURE STUDIES

To support our hypothesis on the anti-tumorigenic effect of NaBt by evoking immunosurveillance system in colorectal cancer, there are number of studies needs to be conducted. Briefly, these include;

* NF-kappaB activity assay for further supporting the DNA-binding activities of p50 and p65 subunits.
* Co-immunoprecipitation assay for the investigation of putative p50 homodimers in the nucleus in response to NaBt treatment.
* Chromatin immunoprecipitation experiments with NF-kappaB canonical subunits for investigation of the promoter regions of inflammation related genes.
* COX-2 enzyme activity assay for further investigation of PGE-2 levels secreted by CRC cells in response to NaBt.
* ELISA for investigation of cytokine secretion by NaBt treated cells.
* Co-culture experiments to investigate leukocyte adhesion to colorectal carcinoma cells differentiated with NaBt.

REFERENCES

Abbas, A. B. & A. H. Lichtman. 2009. *Basic Immunology- Functions and disorders of the immune system.*

Agriculture, U. D. o. 2005. Dietary, Functional and Total Fiber.

Astarci, E., A. Sade, I. Cimen, B. Savas & S. Banerjee (2012) The NF-kappaB target genes ICAM-1 and VCAM-1 are differentially regulated during spontaneous differentiation of Caco-2 cells. *FEBS J.* doi: 10.1111/j.1742-4658.2012.08677.x.

Baeuerle, P. A. & D. Baltimore (1988) I kappa B: a specific inhibitor of the NF-kappa B transcription factor. *Science,* 242**,** 540-6.

Balkwill, F. & A. Mantovani (2001) Inflammation and cancer: back to Virchow? *Lancet,* 357**,** 539-545.

Banno, T., A. Gazel & M. Blumenberg (2005) Pathway-specific profiling identifies the NF-kappa B-dependent tumor necrosis factor alpha-regulated genes in epidermal keratinocytes. *Journal of Biological Chemistry,* 280**,** 18973-18980.

Beg, A. A., W. C. Sha, R. T. Bronson & D. Baltimore (1995) Constitutive NF-kappa B activation, enhanced granulopoiesis, and neonatal lethality in I kappa B alpha-deficient mice. *Genes Dev,* 9**,** 2736-46.

Bingham, S. A., N. E. Day, R. Luben, P. Ferrari, N. Slimani, T. Norat, F. Clavel-Chapelon, E. Kesse, A. Nieters, H. Boeing, A. Tjonneland, K. Overvad, C. Martinez, M. Dorronsoro, C. A. Gonzalez, T. J. Key, A. Trichopoulou, A. Naska, P. Vineis, R. Tumino, V. Krogh, H. B. Bueno-de-Mesquita, P. H. M. Peeters, G. Berglund, G. Hallmans, E. Lund, G. Skeie, R. Kaaks & E. Riboli (2003) Dietary fibre in food and protection against colorectal cancer in the European Prospective Investigation into Cancer and Nutrition (EPIC): an observational study. *Lancet,* 361**,** 1496-1501.

Bocker, U., A. Schottelius, J. M. Watson, L. Holt, L. L. Licato, D. A. Brenner, R. B. Sartor & C. Jobin (2000) Cellular differentiation causes a selective down-regulation of interleukin (IL)-1 beta-mediated NF-kappa B activation and IL-8 gene expression in intestinal epithelial cells. *Journal of Biological Chemistry,* 275**,** 12207-12213.

Brosens, L. A. A., J. J. Keller, G. J. A. Offerhaus, M. Goggins & F. M. Giardiello (2005) Prevention and management of duodenal polyps in familial adenomatous polyposis. *Gut,* 54**,** 1034-1043.

Canani, R. B., M. Di Costanzo, L. Leone, M. Pedata, R. Meli & A. Calignano (2011) Potential beneficial effects of butyrate in intestinal and extrainitestinal diseases. *World Journal of Gastroenterology,* 17**,** 1519-1528.

Carpen, O., P. Pallai, D. E. Staunton & T. A. Springer (1992) Association Of Intercellular-Adhesion Molecule-1 (Icam-1) With Actin-Containing Cytoskeleton And Alpha-Actinin. *Journal of Cell Biology,* 118**,** 1223-1234.

Chang, J., M. R. Chance, C. Nicholas, N. Ahmed, S. Guilmeau, M. Flandez, D. H. Wang, D. S. Byun, S. Nasser, J. M. Albanese, G. A. Comer, B. G. Heerdt, A. J. Wilson, L. H. Augenlicht & J. M. Mariadason (2008) Proteomic changes during intestinal cell maturation in vivo. *Journal of Proteomics,* 71**,** 530-546.

Chen, C. C. & W. A. Walker (2005) Probiotics and prebiotics: role in clinical disease states. *Adv Pediatr,* 52**,** 77-113.

Chen, L. F., W. Fischle, E. Verdin & W. C. Greene (2001) Duration of nuclear NF-kappa B action regulated by reversible acetylation. *Science,* 293**,** 1653-1657.

Cohen, E., I. Ophir & Y. B. Shaul (1999) Induced differentiation in HT29, a human colon adenocarcinoma cell line. *J Cell Sci,* 112 (Pt 16)**,** 2657-66.

Coussens, L. M. & Z. Werb (2002) Inflammation and cancer. *Nature,* 420**,** 860-867.

Creamer, B., R. G. Shorter & J. Bamforth (1961) Turnover And Shedding Of Epithelial Cells .1. Turnover In Gastro-Intestinal Tract. *Gut,* 2**,** 110-&.

Cummings, J. H. (1981) Short Chain Fatty-Acids In The Human-Colon. *Gut,* 22**,** 763-779.

Davie, J. R. (2003) Inhibition of histone deacetylase activity by butyrate. *Journal of Nutrition,* 133**,** 2485S-2493S.

Drori, S., G. D. Girnun, L. Q. Tou, J. D. Szwaya, E. Mueller, X. Kia, R. A. Shivdasani & B. M. Spiegelman (2005) Hic-5 regulates an epithelial program mediated by PPAR gamma. *Genes & Development,* 19**,** 362-375.

Fantini, J., B. Abadie, A. Tirard, L. Remy, J. P. Ripert, A. Elbattari & J. Marvaldi (1986) Spontaneous And Induced Dome Formation By 2 Clonal Cell-

Populations Derived From A Human Adenocarcinoma Cell-Line, HT29. *Journal of Cell Science,* 83**,** 235-249.

Fearon, E. R. & B. Vogelstein (1990) A Genetic Model For Colorectal Tumorigenesis. *Cell,* 61**,** 759-767.

Fox, S. I. 2008. *Human Physiology*. New York: McGraw-Hill.

Frank, P. G. & M. P. Lisanti (2008) ICAM-1: role in inflammation and in the regulation of vascular permeability. *American Journal of Physiology-Heart and Circulatory Physiology,* 295**,** H926-H927.

Fuster, M. M. & J. D. Esko (2005) The sweet and sour of cancer: Glycans as novel therapeutic targets. *Nature Reviews Cancer,* 5**,** 526-542.

Garland, S. H. (2011) Short chain fatty acids may elicit an innate immune response from preadipocytes: A potential link between bacterial infection and inflammatory diseases. *Medical Hypotheses,* 76**,** 881-883.

Ghosh, S. 2007. *Handbook of Transcription Factor NFkappaB*. USA: CRC Press Taylor & Francis Group.

Gibson, G. R. & M. B. Roberfroid (1995) Dietary Modulation Of The Human Colonic Microbiota - Introducing The Concept Of Prebiotics. *Journal of Nutrition,* 125**,** 1401-1412.

Glaser, K. B., M. J. Staver, J. F. Waring, J. Stender, R. G. Ulrich & S. K. Davidsen (2003) Gene expression profiling of multiple histone deacetylase (HDAC) inhibitors: Defining a common gene set produced by HDAC inhibition in T24 and MDA carcinoma cell lines. *Molecular Cancer Therapeutics,* 2**,** 151-163.

Gregorieff, A., D. Pinto, H. Begthel, O. Destree, M. Kielman & H. Clevers (2005) Expression pattern of Wnt signaling components in the adult intestine. *Gastroenterology,* 129**,** 626-638.

Grivennikov, S. I., F. R. Greten & M. Karin (2010) Immunity, Inflammation, and Cancer. *Cell,* 140**,** 883-899.

Harris, R. E. 2007. *Inflammation in the Pathogenesis of Chronic Diseases- The COX-2 Controversy*. New York: Springer.

Horne, R. 1992. Health and Survival in the 21st Century. HarperCollins Publishers Pty Limited.

Huxford, T., D. Mishler, C. B. Phelps, D. B. Huang, L. L. Sengchanthalangsy, R. Reeves, C. A. Hughes, E. A. Komives & G. Ghosh (2002) Solvent exposed non-contacting amino acids play a critical role in NF-kappaB/IkappaBalpha complex formation. *J Mol Biol,* 324**,** 587-97.

Janeway, C. A., J. P. Travers, M. Walport & M. J. Shlomchik. 2004. *Immunobiology*. New York: Garland Science.

Jardillier, J. C. (1981) The Isoenzymes Of The Alkaline-Phosphatases And Their Cancerologic Biochemistries Prospects. *Annales De Biologie Clinique,* 39**,** 115-120.

Ju, J. H., A. S. Naura, Y. Errami, M. Zerfaoui, H. Kim, J. G. Kim, Z. Y. Abd Elmageed, A. B. Abdel-Mageed, C. Giardina, A. A. Beg, M. E. Smulson & A. H. Boulares (2010) Phosphorylation of p50 NF-kappa B at a Single Serine Residue by DNA-dependent Protein Kinase Is Critical for VCAM-1 Expression upon TNF Treatment. *Journal of Biological Chemistry,* 285.

Juliano, R. L. & V. Ling (1976) Surface Glycoprotein Modulating Drug Permeability In Chinese-Hamster Ovary Cell Mutants. *Biochimica Et Biophysica Acta,* 455**,** 152-162.

Kelly, C. P., J. C. Okeane, J. Orellana, P. C. Schroy, S. Yang, J. T. Lamont & H. R. Brady (1992) Human Colon Cancer-Cells Express ICAM-1 Invivo And Support Lfa-1-Dependent Lymphocyte Adhesion Invitro. *American Journal of Physiology,* 263**,** G864-G870.

Khan, A. N. H., C. J. Gregorie & T. B. Tomasi (2008) Histone deacetylase inhibitors induce TAP, LMP, Tapasin genes and MHC class I antigen presentation by melanoma cells. *Cancer Immunology Immunotherapy,* 57**,** 647-654.

Khan, A. N. H., W. J. Magner & T. B. Tomasi (2007) An epigenetic vaccine model active in the prevention and treatment of melanoma. *Journal of Translational Medicine,* 5.

Kien, C. L., J. C. Chang & J. R. Cooper (2000) Butyric acid is synthesized by piglets. *Journal of Nutrition,* 130**,** 234-237.

Kim, H. J. & S. C. Bae (2011) Histone deacetylase inhibitors: molecular mechanisms of action and clinical trials as anti-cancer drugs. *Am J Transl Res,* 3**,** 166-79.

Koshida, K., A. Nishino, H. Yamamoto, T. Uchibayashi, K. Naito, H. Hisazumi, K. Hirano, Y. Hayashi, B. Wahren & L. Andersson (1991) The Role Of Alkaline-Phosphatase Isoenzymes As Tumor-Markers For Testicular Germ-Cell Tumors. *Journal of Urology,* 146**,** 57-60.

Kosinski, C., V. S. W. Li, A. S. Y. Chan, J. Zhang, C. Ho, W. Y. Tsui, T. L. Chan, R. C. Mifflin, D. W. Powell, S. T. Yuen, S. Y. Leung & X. Chen (2007) Gene expression patterns of human colon tops and basal crypts and BMP antagonists as intestinal stem cell niche factors. *Proceedings of the*

National Academy of Sciences of the United States of America, 104**,** 15418-15423.

Leggatt, G. R. & B. Gabrielli (2012) Histone deacetylase inhibitors in the generation of the anti-tumour immune response. *Immunology and Cell Biology,* 90**,** 33-38.

Lehninger, A. L., D. L. Nelson & M. M. Cox. 1993. Principles of Biochemistry. 1090 pp. New York: Worth Publishers.

Li, Z. & G. J. Nabel (1997) A new member of the I kappaB protein family, I kappaB epsilon, inhibits RelA (p65)-mediated NF-kappaB transcription. *Mol Cell Biol,* 17**,** 6184-90.

Lipkin, M. (1965) Cell Replication In Gastrointestinal Tract Of Man. *Gastroenterology,* 48**,** 616-&.

Maeda, K., S. M. Kang, T. Sawada, Y. Nishiguchi, M. Yashiro, Y. Ogawa, M. Ohira, T. Ishikawa & K. H. Y. Chung (2002) Expression of intercellular adhesion molecule-1 and prognosis in colorectal cancer. *Oncology Reports,* 9**,** 511-514.

Mayo, C., J. Lloreta, F. X. Real & X. Mayol (2007) In vitro differentiation of HT-29 M6 mucus-secreting colon cancer cells involves a trychostatinAa and p27(KIP1-) inducible transcriptional program of gene expression. *Journal of Cellular Physiology,* 212**,** 42-50.

Medema, J. P. & L. Vermeulen (2011) Microenvironmental regulation of stem cells in intestinal homeostasis and cancer. *Nature,* 474**,** 318-326.

Meng, X., J. Zhong, S. Liu, M. Murray & A. M. Gonzalez-Angulo (2012) A new hypothesis for the cancer mechanism. *Cancer Metastasis Rev,* 31**,** 247-68.

Methe, B. A., K. E. Nelson, M. Pop, H. H. Creasy, M. G. Giglio, C. Huttenhower, D. Gevers, J. F. Petrosino, S. Abubucker, J. H. Badger, A. T. Chinwalla, A. M. Earl, M. G. FitzGerald, R. S. Fulton, K. Hallsworth-Pepin, E. A. Lobos, R. Madupu, V. Magrini, J. C. Martin, M. Mitreva, D. M. Muzny, E. J. Sodergren, J. Versalovic, A. M. Wollam, K. C. Worley, J. R. Wortman, S. K. Young, Q. Zeng, K. M. Aagaard, O. O. Abolude, E. Allen-Vercoe, E. J. Alm, L. Alvarado, G. L. Andersen, S. Anderson, E. Appelbaum, H. M. Arachchi, G. Armitage, C. A. Arze, T. Ayvaz, C. C. Baker, L. Begg, T. Belachew, V. Bhonagiri, M. Bihan, M. J. Blaser, T. Bloom, V. R. Bonazzi, P. Brooks, G. Buck, C. J. Buhay, D. A. Busam, J. L. Campbell, S. R. Canon, B. L. Cantarel, P. S. Chain, I. M. A. Chen, L. Chen, S. Chhibba, K. Chu, D. M. Ciulla, J. C. Clemente, S. W. Clifton, S. Conlan, J. Crabtree, M. A. Cutting, N. J. Davidovics, C. C. Davis, T. Z. DeSantis, C. Deal, K. D. Delehaunty, F. E. Dewhisrst, E. Deych, Y. Ding, D. J. Dooling, S. P. Dugan, W. M. Dunne, A. S. Durkin, R. C. Edgar, R. L.

Erlich, C. N. Farmer, R. M. Farrell, K. Faust, M. Feldgarden, V. M. Felix, S. Fisher, A. A. Fodor, L. Forney, L. Foster, V. Di Francesco, J. Friedman, D. C. Friedrich, C. C. Fronick, L. L. Fulton, H. Gao, N. Garcia, G. Giannoukos, C. Giblin, M. Y. Giovanni, J. M. Goldberg, et al. (2012) A framework for human microbiome research. *Nature,* 486**,** 215-221.

Morgan, D. W., U. J. Forssman & M. T. Nakada. 2004. *Cancer and inflammation*. Springer Science.

Nakanishi, C. & M. Toi (2005) Nuclear factor-kappa B inhibitors as sensitizers to anticancer drugs. *Nature Reviews Cancer,* 5**,** 297-309.

Niv, Y., J. C. Byrd, S. B. Ho, R. Dahiya & Y. S. Kim (1992) Mucin Synthesis And Secretion In Relation To Spontaneous Differentiation Of Colon Cancer-Cells Invitro. *International Journal of Cancer,* 50**,** 147-152.

Peart, M. J., G. K. Smyth, R. K. van Laar, D. D. Bowtell, V. M. Richon, P. A. Marks, A. J. Holloway & R. W. Johnstone (2005) Identification and functional significance of genes regulated by structurally different histone deacetylase inhibitors. *Proceedings of the National Academy of Sciences of the United States of America,* 102**,** 3697-3702.

Perkins, N. D. (2007) Integrating cell-signalling pathways with NF-kappaB and IKK function. *Nat Rev Mol Cell Biol,* 8**,** 49-62.

Pfaffl, M. W. (2001) A new mathematical model for relative quantification in real-time RT-PCR. *Nucleic Acids Research,* 29.

Pinto, M., S. Robineleon, M. D. Appay, M. Kedinger, N. Triadou, E. Dussaulx, B. Lacroix, P. Simonassmann, K. Haffen, J. Fogh & A. Zweibaum (1983) Enterocyte-Like Differentiation And Polarization Of The Human-Colon Carcinoma Cell-Line Caco-2 In Culture. *Biology of the Cell,* 47**,** 323-330.

Pool-Zobel, B. L. (2005) Inulin-type fructans and reduction in colon cancer risk: review of experimental and human data. *British Journal of Nutrition,* 93**,** S73-S90.

Reya, T. & H. Clevers (2005) Wnt signalling in stem cells and cancer. *Nature,* 434**,** 843-850.

Reynolds, S., S. Rajagopal & S. Chakrabarty (1998) Differentiation-inducing effect of retinoic acid, difluoromethylornithine, sodium butyrate and sodium suramin in human colon cancer cells. *Cancer Letters,* 134**,** 53-60.

Richardson, R. L. & M. Jones (1958) A bacteriologic census of human saliva. *J Dent Res,* 37**,** 697-709.

Roy, C. C., C. L. Kien, L. Bouthillier & E. Levy (2006) Short-chain fatty acids: ready for prime time? *Nutr Clin Pract,* 21**,** 351-66.

Roza, G. 2006. *Inside the human body: using scientific and exponential notation*. New York: Rosen Publishing Group.

Sedgwick, S. G. & S. J. Smerdon (1999) The ankyrin repeat: a diversity of interactions on a common structural framework. *Trends in Biochemical Sciences,* 24**,** 311-316.

Segain, J. P., D. R. de la Bletiere, A. Bourreille, V. Leray, N. Gervois, C. Rosales, L. Ferrier, C. Bonnet, H. M. Blottiere & J. P. Galmiche (2000) Butyrate inhibits inflammatory responses through NF kappa B inhibition: implications for Crohn's disease. *Gut,* 47**,** 397-403.

Segata, N., S. K. Haake, P. Mannon, K. P. Lemon, L. Waldron, D. Gevers, C. Huttenhower & J. Izard (2012) Composition of the adult digestive tract bacterial microbiome based on seven mouth surfaces, tonsils, throat and stool samples. *Genome Biol,* 13**,** R42.

Seitz, C. S., Q. Lin, H. Deng & P. A. Khavari (1998) Alterations in NF-kappa B function in transgenic epithelial tissue demonstrate a growth inhibitory role for NF-kappa B. *Proceedings of the National Academy of Sciences of the United States of America,* 95**,** 2307-2312.

Sen, R. & D. Baltimore (1986) Inducibility Of Kappa-Immunoglobulin Enhancer-Binding Protein Nf-Kappa-B By A Posttranslational Mechanism. *Cell,* 47**,** 921-928.

--- (2006) Multiple nuclear factors interact with the immunoglobulin enhancer sequences (Reprinted from Cell, vol 46, pg 705-716, 1986). *Journal of Immunology,* 177**,** 7485-7496.

Senftleben, U., Y. Cao, G. Xiao, F. R. Greten, G. Krahn, G. Bonizzi, Y. Chen, Y. Hu, A. Fong, S. C. Sun & M. Karin (2001) Activation by IKKalpha of a second, evolutionary conserved, NF-kappa B signaling pathway. *Science,* 293**,** 1495-9.

Shaw, S. K., S. Ma, M. B. Kim, R. M. Rao, C. U. Hartman, R. M. Froio, L. Yang, T. Jones, Y. Liu, A. Nusrat, C. A. Parkos & F. W. Luscinskas (2004) Coordinated redistribution of leukocyte LFA-1 and endothelial cell ICAM-1 accompany neutrophil transmigration. *Journal of Experimental Medicine,* 200**,** 1571-1580.

Simeonidis, S., S. Liang, G. Chen & D. Thanos (1997) Cloning and functional characterization of mouse IkappaBepsilon. *Proc Natl Acad Sci U S A,* 94**,** 14372-7.

Simon-Assman, P., N. Turck, M. Sidhoum-Jenny, G. Gradwohl & M. Kedinger (2007) In vitro models of intestinal epithelial cell differentiation. *Cell Biology and Toxicology,* 23**,** 241-256.

Socransky, S. S. & A. D. Haffajee (2002) Dental biofilms: difficult therapeutic targets. *Periodontology 2000,* 28**,** 12-55.

Tamura, K., Y. Taniguchi, S. Minoguchi, T. Sakai, T. Tun, T. Furukawa & T. Honjo (1995) Physical interaction between a novel domain of the receptor Notch and the transcription factor RBP-J kappa/Su(H). *Current Biology,* 5**,** 1416-1423.

Todaro, M., M. G. Francipane, J. P. Medema & G. Stassi (2010) Colon Cancer Stem Cells: Promise of Targeted Therapy. *Gastroenterology,* 138**,** 2151-2162.

Topping, D. L. & P. M. Clifton (2001) Short-chain fatty acids and human colonic function: Roles of resistant starch and nonstarch polysaccharides. *Physiological Reviews,* 81**,** 1031-1064.

Tureckova, J., M. Vojtechova, D. Kucerova, J. Velek & Z. Tuhackova (2005) Sodium butyrate-mediated differentiation of colorectal cancer cells: Regulation of PKC beta II by PI 3-kinase. *International Journal of Molecular Medicine,* 15**,** 329-335.

Turnbaugh, P. J., V. K. Ridaura, J. J. Faith, F. E. Rey, R. Knight & J. I. Gordon (2009) The Effect of Diet on the Human Gut Microbiome: A Metagenomic Analysis in Humanized Gnotobiotic Mice. *Science Translational Medicine,* 1.

Valeur, J. & A. Berstad (2010) Colonic fermentation: a neglected topic in human physiology education. *Advances in Physiology Education,* 34**,** 22-22.

van der Flier, L. G. & H. Clevers (2009) Stem Cells, Self-Renewal, and Differentiation in the Intestinal Epithelium. *Annual Review of Physiology,* 71**,** 241-260.

van Es, J. H., M. E. van Gijn, O. Riccio, M. van den Born, M. Vooijs, H. Begthel, M. Cozijnsen, S. Robine, D. J. Winton, F. Radtke & H. Clevers (2005) Notch/gamma-secretase inhibition turns proliferative cells in intestinal crypts and adenomas into goblet cells. *Nature,* 435**,** 959-963.

Vinolo, M. A. R., H. G. Rodrigues, E. Hatanaka, C. B. Hebeda, S. H. P. Farsky & R. Curi (2009) Short-chain fatty acids stimulate the migration of neutrophils to inflammatory sites. *Clinical Science,* 117**,** 331-338.

Wanczyk, M., K. Roszczenko, K. Marcinkiewicz, K. Bojarczuk, M. Kowara & M. Winiarska (2011) HDACi - going through the mechanisms. *Frontiers in Bioscience-Landmark,* 16**,** 340-359.

Weih, F., D. Carrasco, S. K. Durham, D. S. Barton, C. A. Rizzo, R. P. Ryseck, S. A. Lira & R. Bravo (1995) Multiorgan Inflammation And Hematopoietic

Abnormalities In Mice With A Targeted Disruption Of RelB, A Member Of The Nf-Kappa-B/Rel Family. *Cell,* 80**,** 331-340.

Wenner, M. 2007. Humans Carry More Bacterial Cells than Human Ones. In *Scientific American*. US.

White, N. R., P. Mulligan, P. J. King & I. R. Sanderson (2006) Sodium butyrate-mediated Sp3 acetylation represses human insulin-like growth factor binding protein-3 expression in intestinal epithelial cells. *Journal of Pediatric Gastroenterology and Nutrition,* 42**,** 134-141.

Whiteside, S. T., J. C. Epinat, N. R. Rice & A. Israel (1997) I kappa B epsilon, a novel member of the I kappa B family, controls RelA and cRel NF-kappa B activity. *EMBO J,* 16**,** 1413-26.

Wolever, T. M. S., R. G. Josse, L. A. Leiter & J. L. Chiasson (1997) Time of day and glucose tolerance status affect serum short-chain fatty acid concentrations in humans. *Metabolism-Clinical and Experimental,* 46**,** 805-811.

Wolter, F. & J. Stein (2002) Resveratrol enhances the differentiation induced by butyrate in Caco-2 colon cancer cells. *Journal of Nutrition,* 132**,** 2082-2086.

Wong, J. M. W., R. de Souza, C. W. C. Kendall, A. Emam & D. J. A. Jenkins (2006) Colonic health: Fermentation and short chain fatty acids. *Journal of Clinical Gastroenterology,* 40**,** 235-243.

APPENDIX A

Optimization of Chromatin Immunoprecipitation Protocol for HT29 Cells

In order to determine the recruitment of NF-kappaB on target gene promoters in the presence or absence of NaBt, a set of chromatin immunoprecipitation (ChIP) experiments were carried out. Before setting up the protocol, several optimization steps were carried out in HT29 cells. As a starting point, different sonication methods (water bath sonicator and probe sonicator) and durations were analyzed for an efficient DNA fragmentation with a target chromatin size of around 500-1000bp, as analyzed by agarose gel electrophoresis containing 1.5% agarose. For water bath sonication, since the sample tube and volume are quite critical, different volumes of samples in different kind of sonication vessels such as 200ul thin-walled tubes, 1.5ml eppendorf tubes or 2ml serological pipette were assayed (Data not shown). Thin-walled tube seemed better for sonication efficiency with 75ul sample volume; much larger volumes were not sonicated efficiently. Probe sonication was better suited for higher volumes and for a 250-400ul volume, showed much better fragmentation. Sonication period up to 15 min were tried, nonetheless, there is almost always some unfragmented intact genomic DNA that were retained in the agarose gel wells. Based on established protocols, a 10 min crosslinking of DNA and proteins with 0.75% formaldehyde is conducted. In order to establish the optimal crosslinking time for HT29 cells, first, sonication was carried out in uncrosslinked DNA samples. For this purpose, DNA purification was carried out by phenol-chloroform extraction from HT29 cells and purified DNA was sonicated and analyzed on 1.5% agarose gel. As can be seen in

Figure A.1 none of the sonicated samples left unsheared genomic DNA in the wells after electrophoresis.

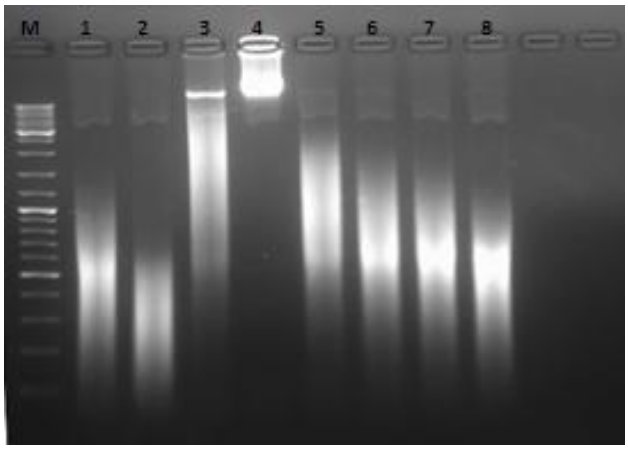

Figure A.1 Optimization of chromatin size in the course of sonication. Phenol-chloroform purified genomic DNA was sonicated under different conditions. Detailed experimental setup for each sample from 1-8 are listed in Table A.1

Table A.1 Experimental setup and sample legend of sonication optimizations.

Cell Sonication Optimization			
Waterbath Sonicator (Default settings-80Hz)			Unsonicated Sample
Continuous 10 min.	Continuous 15 min.	2 min. sonication	-
-	-	30sec. ice	-
-	-	6 cycle	-
50µl sample	50µl sample	50µl sample	-
in 200µl tube	in 200µl tube	in 200µl tube	-
Sample#1	**Sample#2**	**Sample#3**	**Sample#4**
Probe Sonicator (Output Watt:2, Amplitude: 20%)			
10sec. sonication	10sec. sonication	30sec. sonication	30sec. sonication
30sec. ice	30sec. ice	30sec. ice	30sec. ice
5 cycle	10 cycle	5 cycle	10 cycle
250µl sample	250µl sample	250µl sample	250µl sample
in 1,5ml tube	in 1,5ml tube	in 1,5ml tube	in 1,5ml tube
Sample#5	**Sample#6**	**Sample#7**	**Sample#8**

The experimental conditions of sample #8 were observed to be the most suitable regarding the fragment size and homogeneity of sonicated sample. However, the integrity of sonicated protein was still a concern. While increased sonication times could fragment DNA effectively, it could potentially disrupt the 3D structure of proteins and thereby disrupt the epitopes of the protein. This could then affect the recognition of the protein by antibodies and thereby the process of immunoprecipitation. Thus, for assessing the integrity of the protein and epitopes recognized by antibody, a western blot analysis was conducted as explained in Section 2.9, using antibodies that would be used in following chromatin immunoprecipitation experiments. HT29 protein extracts were isolated and sonicated at similar conditions used for DNA sonication. Interestingly, as shown in Figure A.2 the protein of interest was neither fragmented, nor its epitopes were disrupted. In Figure A.2, the last two samples loaded on SDS-PAGE were crosslinked and sonicated samples unlike the other uncrosslinked, pure protein extracts. As can be seen crosslinking was reflected as some smear above protein bands.

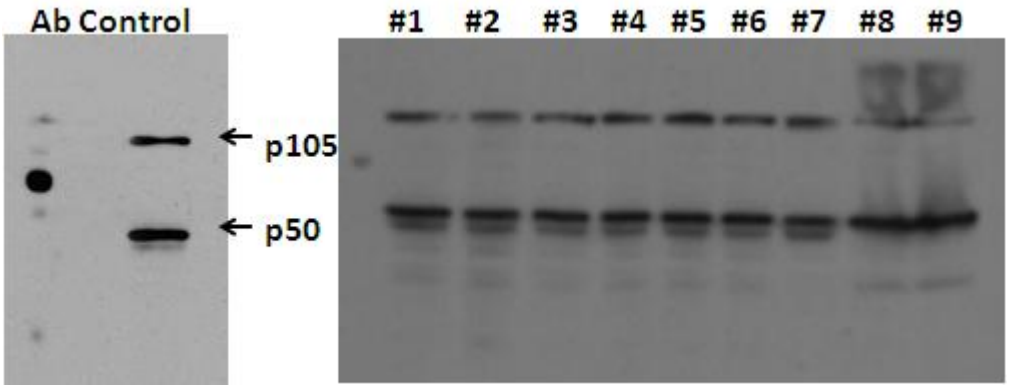

Figure A.2 Checking epitope integrity of TF by western blot analysis. Antibody control western with unsonicated protein extract is indicated to determine whether antibody is recognizing p105 and p50 bands clearly without undergoing non-specific interactions. Detailed legend for numbered samples is provided in Table A.2

Table A.2 Experimental setup and sample legend of sonication optimizations with protein lysate.

Sonication Optimization with Protein Lysate				
Waterbath Sonicator (Default settings-80Hz)			10min Crosslinked & Probe-Sonicated Samples	
Continuous 10 min.	Continuous 15 min.	2 min. sonication	30sec. sonication	30sec. sonication
-	-	30sec. ice	30sec. ice	30sec. ice
-	-	6 cycle	5 cycle	10 cycle
50µl sample	50µl sample	50µl sample	250µl sample	250µl sample
in 200µl tube	in 200µl tube	in 200µl tube	in 1,5ml tube	in 1,5ml tube
Sample#1	**Sample#2**	**Sample#3**	**Sample#8**	**Sample#9**
Probe Sonicator (Output Watt:2, Amplitude: 20%)				
10sec. sonication	10sec. sonication	30sec. sonication	30sec. sonication	
30sec. ice	30sec. ice	30sec. ice	30sec. ice	
5 cycle	10 cycle	5 cycle	10 cycle	
250µl sample	250µl sample	250µl sample	250µl sample	
in 1,5ml tube	in 1,5ml tube	in 1,5ml tube	in 1,5ml tube	
Sample#4	**Sample#5**	**Sample#6**	**Sample#7**	

Following the optimization of the sonication step, the duration of crosslinking was next studies, with incubation with the crosslinker formaldehyde for 30s, 3min or 5min. As can be seen in Figure A.3, image A,B,C as the crosslinking step gets shorter, the DNA seems to be fragmented better, however the concern here was the actual crosslinking of the protein to the DNA. Thus, simultaneously, a western blot experiment was carried out with the crosslinked and sonicated cell lysates, to

assess the minimum incubation time required to crosslink DNA and its binding protein. As can be seen in Figure A.3, image D, up to 3 min of incubation with the crosslinker shows almost no crosslinking. Therefore, the longer durations of incubation with the crosslinker appears to be necessary for efficient cross linking between DNA and protein.

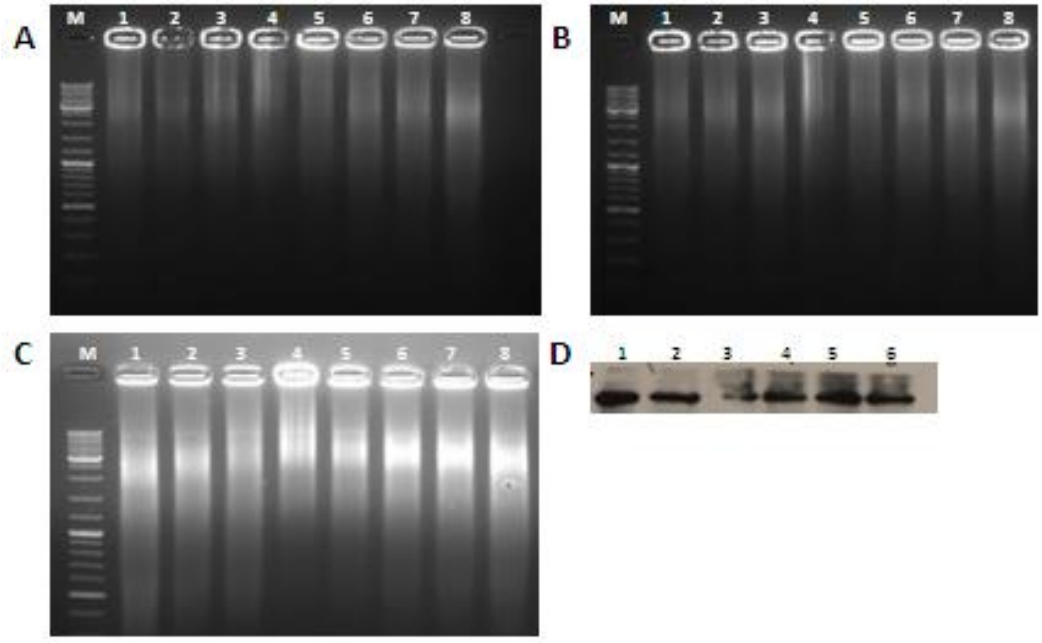

Figure A.3 Optimization of crosslinking time. Chromatin fragment size analysis of A: Crosslinked samples for 5 minutes; B: Crosslinked samples for 3 minutes; C: Crosslinked samples for 30 seconds, explanation related with numbered samples is in Table A.1. D: confirmation of crosslinking by western blot analysis, crosslinked chromatin is represented as retarded smear above protein bands. Samples are 1: uncrosslinked, 2: 30second-crosslinked, 3: 60second-crosslinked, 4: 3minute-crosslinked, 5: 5minute-crosslinked, 6: 10minute-crosslinked cell lysate.

Finally, a cell lysis protocol, which would include a nuclear protein enrichment step prior to sonication, was conducted. For this purpose, pelleted intact cells were

snap-frozen in liquid nitrogen and then immediately thawed in a detergent-free hypertonic solution (Astarci, 2012). Following a centrifugation step to pellet the nuclei, the pellet was resuspended in a lysis buffer containing high amount of detergent. Presence of detergent both enabled the cell lysis and could also affect the efficiency of chromatin fragmentation during sonication since it can promote formation of higher number of air pockets in the suspension. In Figure A.4, image A belongs to the samples that were obtained by nuclear fraction enrichment prior to total lysis and image B belongs to the control samples where this step was not included.

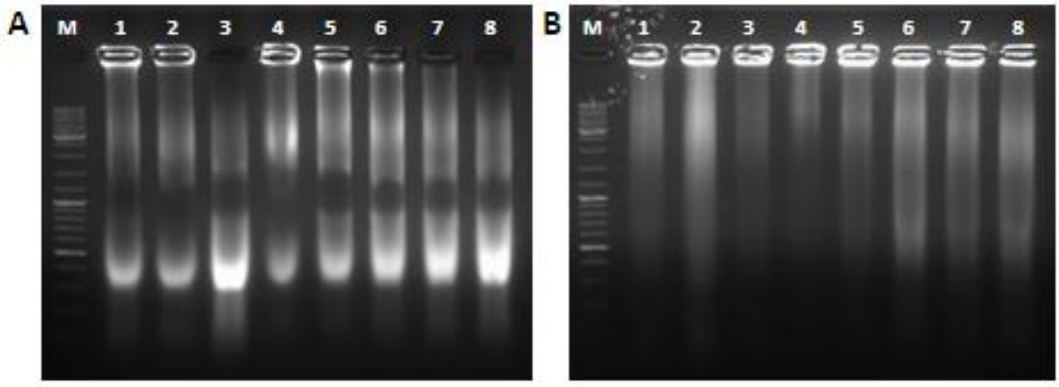

Figure A.4 Optimization of different lysis methods prior to sonication. A: Pelleted cells were snap-frozen and then immediately resuspended in a hypertonic buffer, nuclear pellet was collected after centrifugation and cells were lysed and sonicated in FA lysis buffer (Please see Appendix B for buffer recipies, adapted from "*Abcam ChIP Guide*"), B: Pelleted cells were directly resuspended and then sonicated in FA lysis buffer. For legend of sample numbers please see Table A.1

With this protocol, approximately 400-800bp chromatin fragment size were obtained and the protocol was deemed to be optimized. The crosslinking period was set at 7 minutes, including a nuclear enrichment step prior to total cell lysis and the sonication step was set as 30 second sonication with probe, 30 second incubation on ice with 10 cycles of operation. Based on the *"Abcam Chip Guide"*

and further optimizations with a Histone H3 control antibody, 25ug of chromatin and 10ug of antibody were used per immunoprecipitation vessel.

APPENDIX B

Buffer Recipies

6X Sample Loading Buffer
12% SDS
30% Beta-mercaptaethanol
30% Glycerol
0.012% Bromophenol blue
0.375M Tris HCl pH:6.8

TBS-T
50mM Tris-HCl H:7.4
150mM NaCl
0.1% Tween 20

12% Seperating Gel Mix (for 2 gels)
3.8 ml 10%SDS+1.5M TrisHCl pH 8.8
6.7ml of Acrylamide (30%T)
150 µl APS
20 µl TEMED
4.3 ml dH_2O

4% Stacking Gel Mix (for 2 gels)
2 ml 10%SDS+1.5M TrisHCl pH 6.8
1.2 ml of Acrylamide (30%T)
50 µl APS
10 µl TEMED
4.7 ml dH_2O

SDS-PAGE Buffer
25 mM Tris base
190mM Glycine
0.1% SDS

Transfer Buffer
25 mM Tris base
190mM Glycine
20% Methanol

4% Formaldehyde
4g paraformaldehyde
50ml 2X PBS Buffer pH:7.4
50ml dH_2O

FA Lysis Buffer
50 mM HEPES-KOH pH7.5
140mM NaCl
1mM EDTA pH:8.0
1% Triton X-100
0.1% Sodium Deoxycholate
0.1% SDS
Protease Inhibitor

Buffer A
200M HEPES-KOH pH:7.5
420mM NaCl
0.2mM EDTA pH:8.0
1.5mM $MgCl_2$
25% Glycerol
Protease Inhibitor

Buffer B
50mM Tris-Cl pH:8.0
1mM EDTA pH:8.0
150mM NaCl
1% SDS
2% Triton X-100
Protease Inhibitor

Buffer C
50mM Tris-Cl pH:8.0
1mM EDTA pH:8.0
150mM NaCl
0,1% Triton X-100
Protease Inhibitor

Low-salt Wash Buffer
0.1% SDS
1% Triton X-100
2mM EDTA pH:8.0
150mM NaCl
20mM Tris-HCl pH:8.0

High-salt Wash Buffer
0.1% SDS
1% Triton X-100
2mM EDTA pH:8.0
500mM NaCl
20mM Tris-HCl pH:8.0

SDS Elution Buffer
1% SDS
100mM $NaHCO_3$

APPENDIX C

Primers and Antibodies Used in This Study

Table C. 1 List of Primers Used in This Study

Label	Sequence	Product Size	Tm's	Annealing Target
SB111	GGTGAAGGTCGGAGTCAACG	497bp	57.90	GAPDH mRNA
SB112	CAAAGTTGTCATGGATGACC		51.49	
VillinFwd	AGCCAGATCACTGCTGAGGT	244bp	62,45	Villin mRNA
VillinRev	AGGTTTTGTTGCTTCCATCG		58,35	
Hic5Fwd	GCTAGATCGGTTGCTTCAGG	231bp	62,45	Hic-5 mRNA
Hic5Rev	GCGGAAGTCAGAGAGTGAGG		64,5	
ALPIFwd	GTATGTGTGGAACCGCACTG	243bp	62.45	Alkaline Phosphatase mRNA
ALPIRev	CTGGTAAGCCACACCCTCAT		62.45	
SB190	TCCTTCAGACACCCTCAACC	173bp	56,5	TNF-α mRNA
SB191	AGGCCCCAGTTTGAATTCTT		54,6	
MK-IL1B Forward	AAGTACCTGAGCTCGCCAGTGAAA	169bp	62,7	IL1-β mRNA
MK-IL1B Reverse	TTGCTGTAGTGGTGGTCGGAGATT		62,7	
SB201	CAGAGGTTGAACCCCACAGT	246bp	57,1	ICAM-1 mRNA
SB202	CCTCTGGCTTCGTCAGAATC		55,3	
AS_VCAM_fwd	TTGCTCAGATTGGTGACTCCGTCT	110bp	62.7	VCAM-1 mRNA
AS_VCAM_rev	TTCGTCACCTTCCCATTCAGTGGA		62.7	
ICAM_1_Far_Nf_KBChip_Fwd_	CACTCCCACGGTTAGCGGTCGCCGGGAGGTGC	240bp	> 75	ICAM-1 gene promoter
ICAM_1Far_Nf_kB_Chip_Rev_	GAGACTCCAGGCTGCGAGGGGTCCGAACTC		75.0	

Table C. 2 List of Antibodies Used in This Study

Brand	Catalogue Number	Protein Target	Source/Clonal Status	Epitope	Size
Santa Cruz	*sc-7891*	ICAM-1	Rabbit polyclonal	258-365 at extracellular domain	85-110 kDa
Santa Cruz	*sc-8304*	VCAM-1	Rabbit polyclonal	25-300aa at N-terminus	110kDa
Santa Cruz	*sc-109*	NfKB p65	Rabbit polyclonal	N-terminus of NFκB p65	65kDa
Santa Cruz	*sc-7178*	NfKB p50	Rabbit polyclonal	120-239aa at N-terminus	50kDa
Santa Cruz	*sc-7951*	COX-2	Rabbit polyclonal	50-111aa	70-72kDa
Santa Cruz	*sc-47778*	β-actin	Mouse monoclonal	(not specified in the datasheet)	43-45kDa
Santa Cruz	*sc-10809*	Histone H3	Rabbit polyclonal	1-136aa	15kDa